Stability of Presynaptic Vesicle Pools and Changes in Synapse Morphology in the Amygdala Following Fear Learning in Adult Rats

Linnaea E. Ostroff,[1]* Christopher K. Cain,[1,2] Neha Jindal,[1] Najia Dar,[1] and Joseph E. Ledoux[1,2]

[1]Center for Neural Science, New York University, New York, New York
[2]Emotional Brain Institute, Nathan Kline Institute for Psychiatric Research, Orangeburg, New York

ABSTRACT

Changes in synaptic strength in the lateral amygdala (LA) that occur with fear learning are believed to mediate memory storage, and both presynaptic and postsynaptic mechanisms have been proposed to contribute. In a previous study we used serial section transmission electron microscopy (ssTEM) to observe differences in dendritic spine morphology in the adult rat LA after fear conditioning, conditioned inhibition (safety conditioning), or naïve control handling (Ostroff et al. [2010] Proc Natl Acad Sci U S A 107:9418–9423). We have now reconstructed axons from the same dataset and compared their morphology and relationship to the postsynaptic spines between the three training groups. Relative to the naïve control and conditioned inhibition groups, the ratio of postsynaptic density (PSD) area to docked vesicles at synapses was greater in the fear-conditioned group, while the size of the synaptic vesicle pools was unchanged. There was significant coherence in synapse size between neighboring boutons on the same axon in the naïve control and conditioned inhibition groups, but not in the fear-conditioned group. Within multiple-synapse boutons, both synapse size and the PSD-to-docked vesicle ratio were variable between individual synapses. Our results confirm that synaptic connectivity increases in the LA with fear conditioning. In addition, we provide evidence that boutons along the same axon and even synapses on the same bouton are independent in their structure and learning-related morphological plasticity. J. Comp. Neurol. 520:295–314, 2012.

© 2011 Wiley Periodicals, Inc.

Synaptic plasticity in the lateral amygdala (LA) is believed to underlie learning and memory storage for classical fear conditioning. In fear conditioning, an animal learns to associate a previously neutral conditioned stimulus, often an auditory tone, with an aversive unconditioned stimulus, typically a mild footshock (LeDoux, 2000; Maren, 2001; Fanselow and Poulos, 2005). This association persists for the life of the animal, and its storage is permanently dependent on the LA (Gale et al., 2004). Auditory brain areas project directly to the LA and fear conditioning to a tone enhances tone-evoked field potentials, cell firing, and synaptic strength in the LA (Quirk et al., 1995; McKernan and Shinnick-Gallagher, 1997; Rogan et al., 1997). LA synapses are thus functionally plastic; in addition, fear conditioning shares a constantly growing assortment of cellular and molecular mechanisms with LA synaptic plasticity (LeDoux, 2000; Blair et al., 2001; Rodrigues et al., 2004; Fanselow and Poulos, 2005; Sah et al., 2008). Fear conditioning is the best example to date of a direct link between learning and synaptic plasticity in the vertebrate forebrain, making the LA uniquely suited for studies of synaptic mechanisms underlying learning and memory (Barnes, 1995; Stevens, 1998; Sah et al., 2008).

During fear conditioning training, footshocks are preceded by auditory tones so that the animal learns that the tone predicts the footshock. Thereafter, the tone elicits fearful behavioral responses. In conditioned inhibition, a related procedure, the tones and footshocks are explicitly nonoverlapping so that the animal learns to associate the tone with safety from the footshock. After

conditioned inhibition training, the tone suppresses fearful behavioral responses (Rescorla, 1969). It is therefore possible to train animals to form different fear associations to the same cue. Significantly, unlike appetitive or instrumental associations, conditioned inhibition can be learned in a single session using the same number of tones and footshocks as fear conditioning (Ostroff et al., 2010). Tone-evoked field potentials in the LA are reduced after conditioned inhibition and enhanced after fear conditioning, indicating that synaptic responses as well as behavioral fear responses are bidirectionally altered by these two training procedures. This allows not only fear associations, but the valence of fear associations to be examined at the synaptic level.

Synapse structure is dynamic at both the morphological and molecular levels, and structural plasticity is generally believed to be involved in learning and memory (Bourne and Harris, 2007; Kasai et al., 2010). Like nearly all forms of learning that have been studied, the formation of long-term memory of fear conditioning requires the synthesis of new proteins. Inhibition of protein synthesis or a number of related processes in the first few hours after learning prevents the formation of long-term memory, but leaves short-term memory intact. This stabilization process is called consolidation, and since several synaptic proteins are known to be synthesized it is easy to imagine that the new proteins support structural changes at synapses (Barondes and Squire, 1972; Davis and Squire, 1984; Schafe et al., 1999, 2000; Schafe and LeDoux, 2000; Sutton and Schuman, 2006; Hernandez and Abel, 2008; Klann and Sweatt, 2008). The consolidation period is thus a particularly interesting timepoint at which to examine synapse structure.

Dendritic spine structure has been studied extensively in hippocampus and cortex using in vitro plasticity paradigms, and more recently live imaging of cortical spines has been employed during learning in intact animals (Alvarez and Sabatini, 2007; Bourne and Harris, 2008; De Roo et al., 2008; Holtmaat and Svoboda, 2009; Xu et al., 2009; Yang et al., 2009; Kasai et al., 2010). One study has described the calcium dynamics of LA spines in vitro, but the LA is a deep brain structure and thus cannot be optically imaged in vivo during learning using current techniques (Humeau et al., 2005). Using serial section transmission electron microscopy (ssTEM), we have found that fear conditioning and conditioned inhibition produce bidirectional changes in the size of dendritic spines and synapses in the LA during the consolidation period (Ostroff et al., 2010).

Synaptic plasticity in the LA involves changes in presynaptic as well as postsynaptic function, raising the possibility that presynaptic structure may also change with learning (Sigurdsson et al., 2007; Sah et al., 2008). Very few studies have examined axon and bouton structure during learning, although there is evidence that they, too, are dynamic

under plasticity conditions (Gogolla et al., 2007). Forebrain boutons are motile and turn over under baseline conditions, and the turnover rate is enhanced by activity (De Paola et al., 2003, 2006; Konur and Yuste, 2004; Umeda et al., 2005; Stettler et al., 2006; Becker et al., 2008; Lin et al., 2010; Marik et al. 2010). Dendritic spines and boutons also have characteristic morphological relationships to each other under baseline conditions, but whether these relationships are dynamic is unknown (Schikorski and Stevens, 1997; Shepherd and Harris, 1998). To determine whether learning alters presynaptic morphology in the LA, we used ssTEM to reconstruct axons from rat LA during consolidation of fear conditioning or conditioned inhibition, or after naïve control handling. Axons were reconstructed from an existing ssTEM dataset whose dendritic morphology had already been analyzed (Ostroff et al., 2010). We were therefore able not only to compare presynaptic morphology between training groups, but to determine relationships between presynaptic and postsynaptic elements as well.
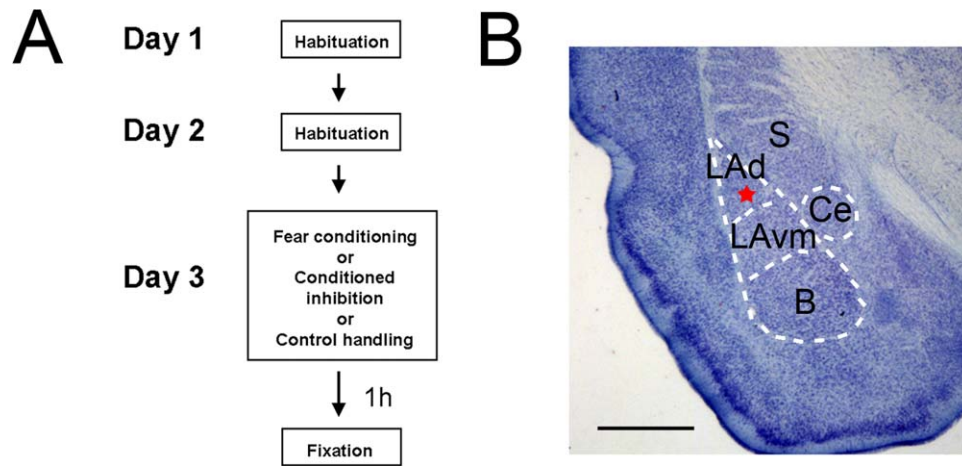
MATERIALS AND METHODS

Analyses were performed on existing serial electron micrographs from a previous study (Ostroff et al., 2010). All procedures were approved by New York University's Animal Care and Use Committee.

Subjects

Subjects were adult male Sprague–Dawley rats weighing ≈300 g (Hilltop Lab Animals, Scottdale, PA). Rats were housed singly on a 12-hour light/dark cycle and allowed free access to food and water. Experiments were conducted during the animals' light cycle, and all training sessions began between 9 AM and 11:30 AM.

Behavior

Training took place in standard Coulbourn fear conditioning chambers (28.5 × 26 × 28.5 cm; Model E10-10; Whitehall, PA). Scrambled footshocks (1 sec, 0.7 mA) were delivered through grid floors and tones (30 sec, 80 dB, 5 kHz) were delivered via speakers mounted in the walls (1/chamber). The training sequence is shown in Figure 1A. All rats were habituated to the Coulbourn chambers for 2 days (30 min/day) prior to training. The naïve group (n = 3) received handling and exposure to the chamber on the habituation and training days identical to the two conditioned groups, but was given no shocks or tones. Conditioned rats were trained using protocols designed to produce either fear conditioning (FC, n = 3) or conditioned inhibition (CI, n = 3) to the tone. Five tones and five shocks were given to both groups over 32.5 minutes and the temporal placement of the tones was identical for all rats. For FC rats, each tone coterminated with a footshock, while for CI rats footshocks were

Figure 1. Methods. **A:** Flow chart of behavioral training (see Materials and Methods). **B:** Nissl-stained coronal section showing amygdala nuclei. Red star indicates the source of tissue samples. LAd, dorsolateral amygdala; LAvm, ventromedial lateral amygdala; Ce, central extended amygdala; B, basal amygdala; S, ventral striatum. Scale bar = 1 mm.

interleaved with tones in an explicitly unpaired manner, occurring on average 2 minutes before each tone. On the training day both groups were placed in the dimly lit Coulbourn chambers and allowed to acclimate for 5 minutes before the first tone or shock. The mean intertrial interval (ITI) for tone-shock pairings in the FC protocol was 5 minutes; in the CI protocol the mean shock-to-tone interval was 119 seconds and the mean tone-to-shock interval was 180 seconds. Rats were removed from the chambers 5 minutes following the last tone. Diagrams of these protocols and experiments demonstrating that they produce long-term fear and safety associations, as well as naïve controls confirming that the rats in this study showed normal fear or safety acquisition have been published previously (Ostroff et al., 2010).

Tissue preparation

One hour after the first shock delivered during training (or an equivalent timepoint for naïve rats), rats were deeply anesthetized with chloral hydrate (1 g/kg intraperitoneal) and perfused transcardially with ≈50 cc of heparinized saline followed by 500 ml of 2.5% glutaraldehyde/2% paraformaldehyde in 0.1M phosphate buffer (pH 7.4). All animals were perfused within 1 month of each other, with at least two brains collected on each of 4 perfusion days. Brains were removed and sat at room temperature in perfusion fix for ≈2 hours prior to being sectioned coronally at 70 μm on a vibrating slicer (Leica). The area of tissue around the left LA was dissected out using a fine knife and rinsed in phosphate buffer. All processing took place at room temperature except resin curing. Sections were incubated in potassium ferrocyanide-reduced osmium (1.5% potassium ferrocyanide/1% osmium in 0.1M phosphate buffer) for 1 hour, rinsed in buffer, and then fixed in 1% osmium (Electron Microscopy Sciences, Fort Washington, PA) for an additional hour. After rinses in buffer and water, sections were dehydrated in a series of graded aqueous ethanols for 10 minutes each (50%/70%/90%/2×100%), each of which contained 1% uranyl acetate (Electron Microscopy Sciences). Tissue was then rinsed in pure ethanol and transferred in steps to acetone, then infiltrated for 1 hour in a 1:1 mix of acetone to LX-112 resin (Ladd Research, Burlington, VT). Following overnight incubation in a 1:4 acetone:LX-112 mix, tissue sections were embedded in flat coffin molds and cured at 60°C for 48 hours.

Serial sectioning and electron microscopy

Resin blocks containing sections of LA approximately midway along its rostral-caudal axis were trimmed by hand using a razor blade to expose the area of the LA just below the dense fiber bundles of the dorsolateral subregion of the LA (LAd). A schematic of the LA and the sampled area is shown in Figure 1B. Serial sections were cut at 45 nm on an Ultracut U microtome (Leica) as previously described (Harris et al., 2006). Series ribbons of ≈200 sections were collected on pioloform-coated single-slot Synaptec grids and stained with saturated uranyl acetate and Reynold's lead citrate stain. One series per rat (range 120–160 sections, mean 143) was photographed on a JEOL 1200EX electron microscope at a magnification of 7,500× (field size ≈10 × 12 μm), and negatives were developed and digitized using a flat bed scanner (Epson).

Serial reconstruction and structural analysis

Reconstruct software was used to align digitized images and perform all measurements (Fiala, 2005), and all analysis was done with the experimenters blind to training group. Section thickness was determined using

mitochondrial diameters (Fiala and Harris, 2001). All measurements were made through serial sections. Postsynaptic density (PSD) area for cross-sectioned PSDs was quantified as the summed lengths of PSD profiles on each single section multiplied by the section thickness. Rare, completely obliquely sectioned PSDs were measured on a single section; these were identifiable by an obvious intensely stained area with a spine head on one adjacent section and presynaptic vesicles on the other (Kubota et al., 2009). For PSDs sectioned at near-oblique angles, the extra area was accounted for on the individual section measurements by measuring both section thickness and oblique area. Docked vesicles could not be unambiguously identified if the presynaptic membrane was obscured by the PSD due to section angle, and synapses were excluded if this was the case. Images of 3D reconstructions were rendered in 3DS Max (Autodesk). Photomicrographs in the figures were cropped and brightness and contrast adjusted in Adobe Photoshop (San Jose, CA).

Sampling and composition of the dataset

Two sets of boutons were sampled from an existing set of reconstructed ssTEM volumes The first set consisted of all boutons presynaptic to asymmetric synapses on dendrites analyzed in a previous study (Ostroff et al., 2010). Asymmetric synapses were characterized by the presence of round synaptic vesicles in apposition to a PSD, in contrast to the pleomorphic vesicles and absence of a prominent PSD at symmetric synapses (Gray, 1959a,b). Boutons were only included in the analysis if their entire 3D morphology was complete in the series; 891 (387 FC, 317 naïve, 187 CI) boutons met this requirement. A set of axon segments was also sampled and the boutons on these axons ($n = 311$ boutons; 109 FC, 95 naïve, 105 CI) were also included. The number differs between groups in the dataset taken from the dendrites because the synapse frequency on dendrites differed between groups.

Axon segments containing multiple boutons were selected in an unbiased manner. All profiles on the tenth section from the ventral end of each series were examined through serial sections and all those that proved to be boutons were selected for further analysis. The entire extent of each axon of each of these boutons was followed through the series. Axons with at least two complete boutons contained in the series were included in the dataset. The exceptions were axons containing large (≥ 100 nm) dense-core vesicles and axons forming symmetric synapses; these were excluded. No axon was found to form both symmetric and asymmetric synapses. This selection procedure yielded 142 axon segments making asymmetric synapses onto dendrites (47 FC, 45 naïve, 50 CI). The LAd is a nuclear structure with no apparent histological organization, and its afferent axons run in all orientations. We

began our sampling near the end of the series to maximize our chances of finding axons with multiple boutons in the series. Since our tissue volume width (7×12 μm) is larger than the height (≈ 6 μm), axons traversing diagonally or horizontally were somewhat more likely to meet the selection criteria than directly vertical axons.

Statistics

Means were compared using analysis of variance (ANOVA). Means of individual boutons, axons, or PSDs were used for analysis, but a hierarchical ANOVA design was used with animal nested into group to account for the identity of the animal in each measurement. Significant interactions ($P < 0.05$) were not observed between group and animal for the data reported. If significant effects ($P < 0.05$) were found in the overall ANOVA, the Fisher Protected LSD test was used to compare the naïve group to each of the trained groups and these are the P values reported. Since we were interested in the differences between animals that learned and those that did not, we did not directly compare the FC and CI groups. Where data were compared by factors other than training group, the Bonferroni procedure was used and the effect is stated. Post-hoc P values are reported. ANOVAs were only used on normally distributed data, or on log-normal data subjected to a logarithmic transformation before analysis. These data are presented as bar graphs showing means $\pm$ standard error of the mean. In instances where it is stated that a measure was not changed between training groups or for analyses in which multiple groups were collapsed, a factorial ANOVA was used to ensure that there were no significant interactions between groups and independent variables. Kruskal–Wallis ANOVA by ranks was used to compare nonnormal distributions; these data are presented as histograms. Correlations are simple regression and R^2 is reported only for $P < 0.05$.

Although all boutons in the dataset were entirely contained in the series, not every measurement could be taken from every bouton. For example, on synapses sectioned at oblique or near-oblique angles it was often impossible to confidently quantify docked vesicles. Only 809 out of 1,202 boutons had complete information on all measures analyzed in the study. All 1,202 boutons were used to maximize statistical power, which means that a slightly different subpopulation was used in each analysis. However, restricting each analysis to the 809 complete boutons produced similar results, although these results did not always reach statistical significance due to lower numbers.

RESULTS

Putative origin of axons in LAd

In order to preserve ultrastructure and avoid obscuring any organelles in the neuropil, including vesicles, we did

not use any tracers or labels to identify the source of axons in our material since the fixation and visualization processes severely compromise ultrastructure. However, enough is known about the projections to the LA to limit the possible sources to a few cortical and thalamic areas. The majority of neurons in the LA are glutamatergic projection cells with pyramidal-like somata and spiny dendrites (McDonald, 1982; McDonald, 1992). The remaining cells are nonpyramidal GABAergic interneurons with aspinous or sparsely spiny dendrites (McDonald, 1982; McDonald and Pearson, 1989). All of the axons in our dataset formed synapses with spiny dendrites, meaning that they are all presynaptic to pyramidal cells. Glutamatergic synapses in the LA are asymmetric, while GABAergic, dopaminergic, and serotonergic synapses are largely symmetric (Farb et al., 1992; McDonald et al., 2002; Muller et al., 2006, 2007a,b, 2009). Acetylcholine receptors are expressed in LAd (i.e., Seguela et al., 1993; McDonald and Mascagni, 2010), and although their morphology has not been studied in LAd, cholinergic synapses in basal amygdala, cortex, and striatum are known to be symmetric (Houser et al., 1985; Phelps et al., 1985; Li et al., 2001). Noradrenergic axons do form some asymmetric synapses in the LA, but about two-thirds of their synapses are symmetric. They also can contain large dense-core vesicles (Farb et al., 2010). Because we only sampled axons making exclusively asymmetric synapses and lacking large dense-core vesicles, it is likely that our dataset is composed mostly of glutamatergic axons.

Dendrites on pyramidal neurons in the dorsolateral region of the rat LAd form synapses with axons from a number of brain areas. Axons from the auditory thalamus, specifically the medial division of the medial geniculate nucleus (MGm) and the neighboring posterior intralaminar nucleus (PIN), as well as the auditory association area TE3 are known to form excitatory asymmetric synapses on LAd spines and dendrites (LeDoux et al., 1991a; Farb and LeDoux, 1997, 1999). No other thalamic areas have been observed to project heavily to the LA (LeDoux et al., 1990, 1991b). Several other cortical areas project to LAd, including regions of perirhinal, entorhinal, insular, and occipital cortex (LeDoux et al., 1991b; Mascagni et al., 1993; McDonald and Mascagni, 1996, 1997; Shi and Cassell, 1998a,b, 1999). Although no information is available on the synaptic morphology of projections from nonauditory areas, it is probable that they, like other cortical axons, form asymmetric synapses on dendritic spines. Unlike most other regions of the amygdala, LAd receives almost no input from the rest of the amygdala (Pitkanen et al., 1997). Based on the available data, it is reasonable to expect that the axons in our study originate mainly from posterior thalamic and temporal cortical areas containing neurons that process auditory signals.

Morphological vesicle pools are stable and correlated

Synaptic vesicles can be sorted into separate pools both functionally and morphologically. Functionally, the readily releasable pool is a subset of vesicles that are available to release neurotransmitter at the synapse within seconds (Stevens and Tsujimoto, 1995; Rosenmund and Stevens, 1996; Sudhof, 2004; Schweizer and Ryan, 2006). The size of the readily releasable pool is equal to the number of morphologically docked vesicles, which interact directly with the active zone (Schikorski and Stevens, 2001). The vast majority of synaptic vesicles are not docked at the synapse but comprise the reserve pool, which functionally may include further subsets of vesicles that are mobilized in turn when the readily releasable pool is depleted (Sudhof, 2004; Rizzoli and Betz, 2005; Schweizer and Ryan, 2006). We counted all synaptic vesicles in both pools through serial sections for each bouton in our dataset.

Boutons en passant were observed morphologically as swellings containing small round synaptic vesicles (≈ 50 nm in diameter) along otherwise narrow lengths of axons. There were no terminaux boutons in our dataset. No boutons were found without vesicles, although stray vesicles were occasionally seen between boutons along an axon. Docked vesicles were defined morphologically as being within 10 nm of an active zone in apposition to a PSD. All other vesicles were defined as comprising the reserve pool. The reserve pool was measured only where vesicles could be clearly counted through the entire bouton, and only in boutons that were contained entirely within the tissue volume to avoid undercounting. Docked vesicles were counted only at synapses where their identity could be clearly confirmed. Figure 2A,B shows examples of synaptic vesicles at synapses. In naïve rats the reserve pool contained on average 454 ± 31 vesicles, and this number was not significantly different in the trained groups (Fig. 2C). The reserve pool mean is noticeably (but insignificantly) smaller FC group; this is accounted for below in Figures 3E and 8G. The number of docked vesicles in each bouton was also similar among groups, averaging 5.3 ± 0.4 in the naïve group (Fig. 2D). Docked vesicle number was significantly correlated with reserve pool size in all three training groups (Fig. 2E).

Synapse morphology changes with fear conditioning and conditioned inhibition

Fear learning is known to change LA synapse function, with stronger and weaker synapses observed after fear conditioning and conditioned inhibition, respectively (Rogan and LeDoux, 1995; McKernan and Shinnick-Gallagher, 1997; Rogan et al., 2005; Pollak et al., 2008).
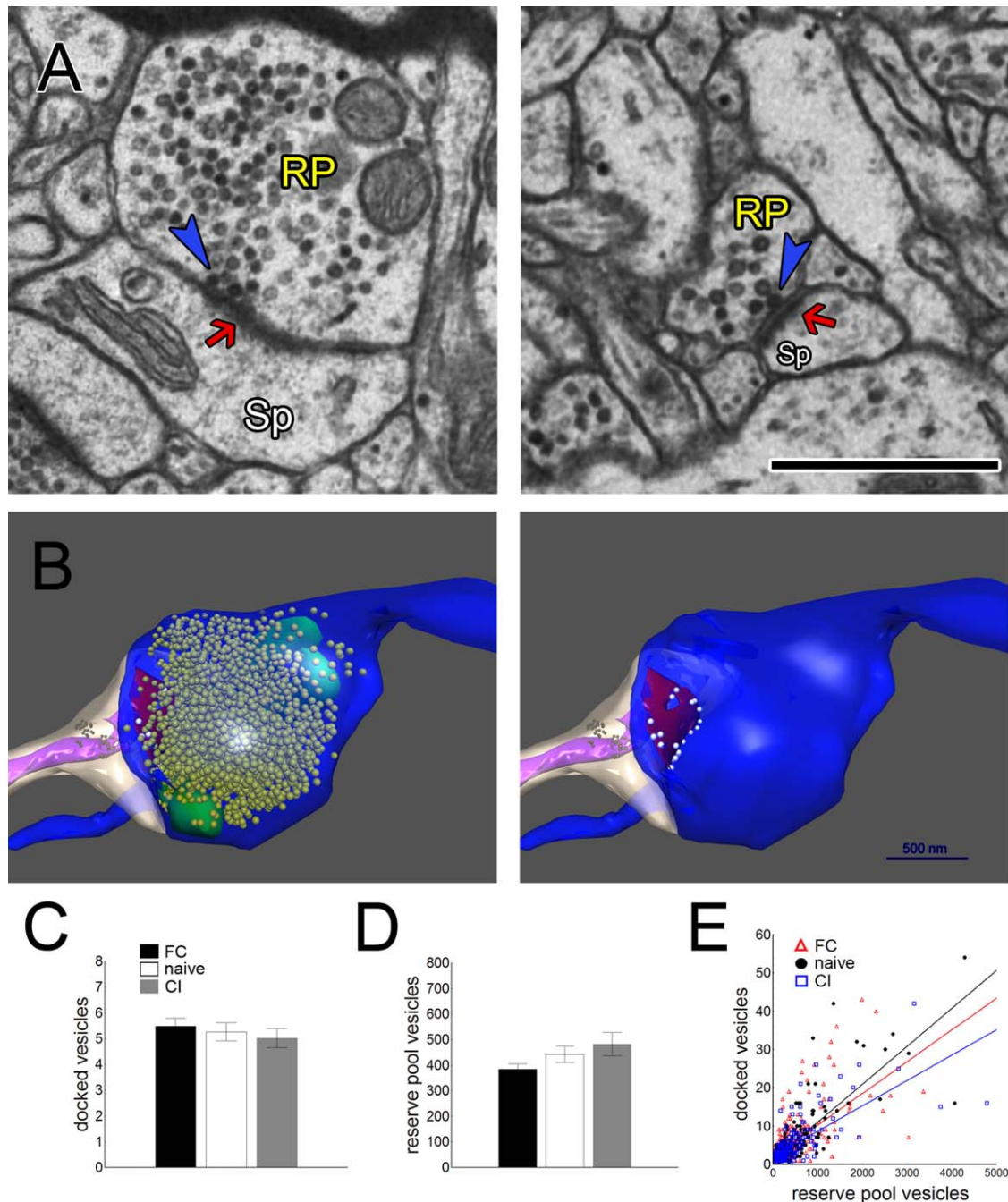
Figure 2. Vesicle pools are morphologically coupled. **A:** Transmission electron micrographs of a lateral amygdala synapses. The dendritic spines (Sp), postsynaptic densities (red arrows), reserve pools (RP), and docked vesicles (blue arrowhead) are indicated. **B:** Left: reconstructed bouton (blue) forming a synapse (red) on a dendritic spine (gray). Reserve pool vesicles are in yellow, docked vesicles are in white, and mitochondria are in green, the spine apparatus is in purple, and ribosomes are in black. Right: the same bouton showing only the docked vesicles. **C:** Fear learning does not change the number of reserve pool vesicles ($P = 0.07$). FC $n = 418$, naïve $n = 312$, CI $n = 232$. **D:** Fear learning does not change the number of docked vesicles ($P = 0.9$). FC $n = 566$, naïve $n = 418$, CI $n = 326$. **E:** The reserve pool and docked vesicle pool are correlated in all groups (FC: $R^2 = 0.42$; naïve: $R^2 = 0.65$, CI: $R^2 = 0.74$). Scale = 1 μm in A.

Structural changes have been observed on the postsynaptic side, including glutamate receptor insertion after fear conditioning and bidirectional changes in dendritic spine size with fear conditioning and conditioned inhibition (Rumpel et al., 2005; Ostroff et al., 2010). Synaptic adhesion molecules in the LA are involved in fear conditioning, suggesting that both sides of the synapse are altered (Maguschak and Ressler, 2008; Bisaz and Sandi, 2010). We looked at PSD area with respect to the presynaptic bouton, as the active zone is not reliably visible in
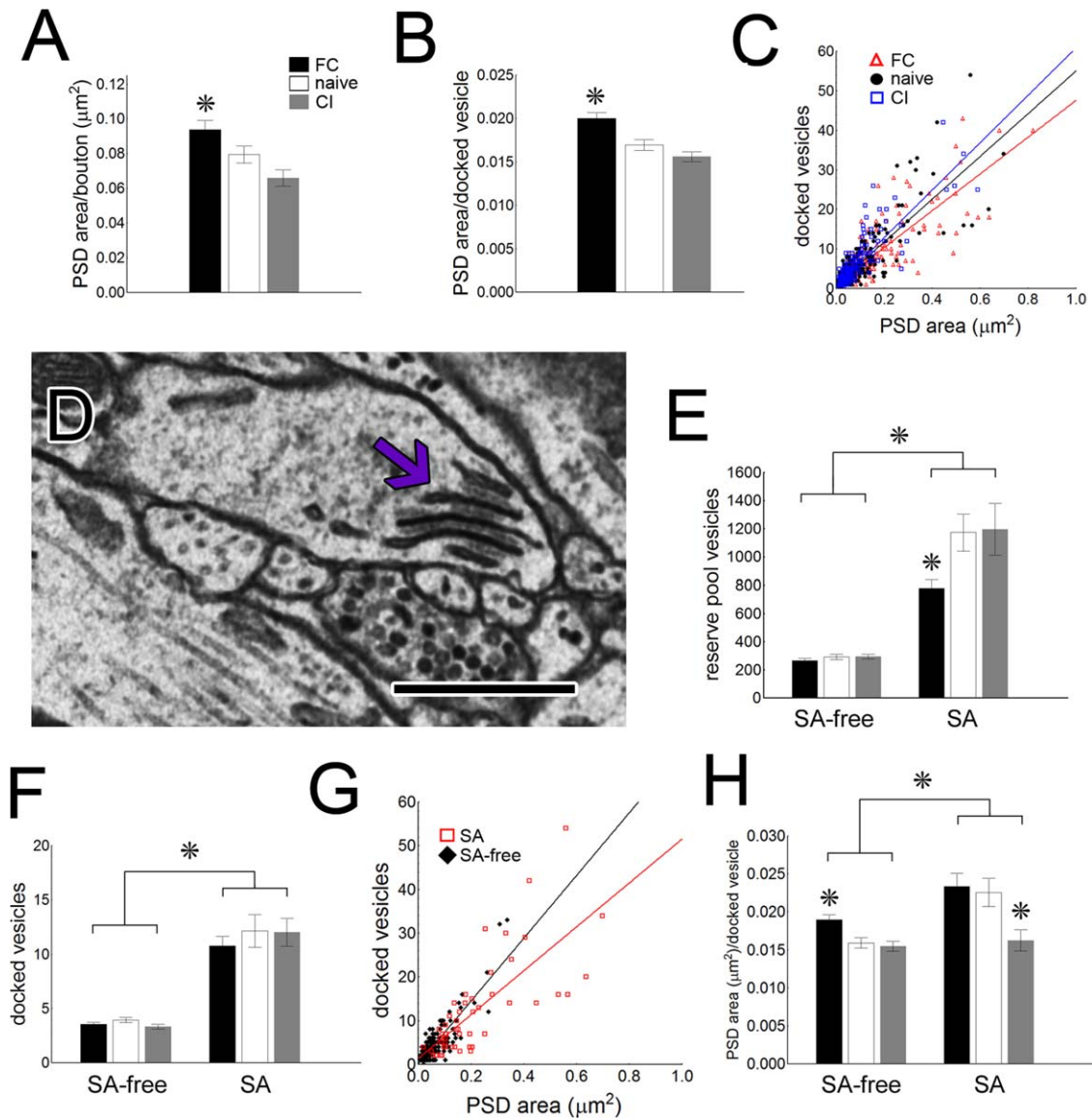
Figure 3. A: The area of PSD on each bouton increases with fear conditioning. FC $n = 615$, naïve $n = 491$, CI $n = 343$ (*$P < 0.005$).
B: The ratio of PSD to docked vesicles increased with fear conditioning. FC $n = 536$, naïve $n = 412$, CI $n = 311$ (*$P < 0.0005$).
C: Docked vesicle number correlates with PSD area in all groups (FC: $R^2 = 0.71$; naïve: $R^2 = 0.69$, CI: $R^2 = 0.73$). **D:** Electron micrograph
of a spine apparatus (arrow) in a dendritic spine. **E:** There are more reserve pool vesicles on boutons presynaptic to a spine apparatus,
but the reserve pool is smaller in the FC group if a spine apparatus is present (*$P < 0.001$). SA-free: FC $n = 285$, naïve $n = 238$, CI $n = $
170; SA: FC $n = 100$, naïve $n = 50$, CI $n = 45$. **F:** There are more docked vesicles at synapses with a spine apparatus (*$P < 0.0001$).
G: Regardless of the presence of a spine apparatus (SA), docked vesicle number correlates with PSD area (naïve group shown; SA: $R^2 = $
0.55, SA-free $R^2 = 0.73$). **H:** The PSD-to-docked vesicle ratio is higher overall at synapses with an associated spine apparatus. SA-free:
FC $n = 378$, naïve $n = 309$, CI $n = 235$; SA: FC $n = 126$, naïve $n = 65$, CI $n = 59$. The ratio on SA versus SA-free spines is significantly
different in the FC and naïve groups only ($P < 0.001$, bars not marked for clarity). FC and CI are different from naïve in the SA-free and
SA groups, respectively (*$P < 0.01$). Legend in A applies throughout. Scale bar $= 500$ nm.

our preparation. To determine whether the synaptic connectivity on individual boutons was affected by learning, we measured the area of each PSD in two dimensions. The FC group had a higher average PSD area per bouton (Fig. 3A). The smaller mean PSD area in the CI group relative to the naive is not significant ($P = 0.09$); Figure 7F revisits this. Docked vesicle number was not significantly different between groups, and accordingly the ratio of PSD area to docked vesicles was higher in the FC group relative to the naïve group (Fig. 3B). Docked vesicle number was correlated with PSD area in all training groups (Fig. 3C), as has been reported in the hippocampus as well (Harris and Sultan, 1995; Schikorski and Stevens, 1997).

Our measurements of docked vesicle number and PSD area demonstrate that during the initial consolidation period of fear conditioning the FC group had a different morphological relationship between the presynaptic and postsynaptic elements. The major structural change in dendritic spines associated with fear conditioning is a higher frequency of spines with a spine apparatus (Ostroff et al., 2010). This understudied organelle occurs in the largest 20% of dendritic spines and is composed of membranous cisterns interleaved with dense plates (Fig. 3D). Perforated PSDs, which are very large and have an irregular shape, often containing fenestrations or discontinuities (i.e., Fig. 6A), occur in 60% of spines with a spine apparatus and only 2% of other spines (66 of 164 and 16 of 788, respectively).

To determine whether the morphological composition of synapses varies with spine structure, we analyzed boutons with respect to the presence of a postsynaptic spine apparatus. In the naïve group the PSD area on spines with a spine apparatus is six times larger than other spines, making this an enormous morphological class (Ostroff et al., 2010). Likewise, boutons presynaptic to a spine apparatus had ≈6 times as many reserve pool vesicles. In the FC group, however, boutons presynaptic to a spine apparatus had smaller reserve pools (Fig. 3E). These observations indicate a morphological coupling between the PSD and the reserve pool. A possible explanation for the smaller reserve pool size in the FC group is that smaller spines may enlarge with fear conditioning and add a spine apparatus, while the reserve pool enlarges on a longer time scale.

Synapses with a spine apparatus had ≈3 times more docked vesicles than other spines in all training groups (Fig. 3F). Although PSD area and docked vesicle number are generally correlated, it is clear that where the spine apparatus is concerned the presynaptic and postsynaptic elements do not scale linearly. However, the correlation between PSD area and docked vesicles still holds for each group (Fig. 3F). In the naïve and FC groups there was a significantly higher PSD-to-docked vesicle ratio when a spine apparatus was present (Fig. 3G). CI boutons had significantly smaller PSDs than naïve boutons when a postsynaptic spine apparatus was present (naïve 0.21 ± 0.01 μm^2; CI 0.17 ± 0.01 μm^2, $P < 0.002$). Accordingly, there was a higher PSD-to-docked vesicle ratio on SA-free spines in the FC group and a smaller ratio on SA spines in the CI group (Fig. 3H).

New, potentially local protein synthesis is required for consolidation of fear conditioning during the timepoint we tested (Helmstetter et al., 2008). We reported previously that polyribosomes (sites of protein synthesis) are upregulated in dendritic spines in the FC group and that spines with polyribosomes generally have larger PSDs (Ostroff

et al., 2010). To determine whether this was also true of presynaptic vesicles, we examined the reserve pools in our boutons with respect to postsynaptic polyribosomes (Fig. 4A). No polyribosomes were observed in the axons. In boutons presynaptic to spines lacking a spine apparatus there was no difference in reserve pool size between groups or when polyribosomes were present. On the other hand, boutons presynaptic to spines with a spine apparatus had larger reserve pools in the naïve group if polyribosomes were present. This was not the case in the FC or CI groups. When polyribosomes were present the reserve pool was smaller in the FC group than in the naïve group, which accounts for the difference seen in Figure 3E. In the CI group the reserve pool was larger than in the naïve group when polyribosomes were not present (Fig. 4B). The docked vesicle pool was also smaller in the FC group when a spine apparatus and polyribosomes were present.

Bouton coherence and synapse independence along axons

Unlike spines along a dendrite, which generally are each contacted by different axons and therefore receive different activity patterns, boutons along an axon all experience the same pattern of action potentials. Even so, bouton function is not necessarily uniform. Boutons along the same axon have been observed to exhibit different release probabilities, calcium dynamics, and types of plasticity (Pelkey and McBain, 2007). In order to compare morphology between boutons along individual axons, we reconstructed axon segments that formed at least two boutons (mean 2.5 ± 0.7, maximum 5) with synapses on spiny dendrites (Fig. 5A,B). The average distance between boutons was 2.5 μm in the naïve group and did not change with training, although there was a nonsignificant difference between the naïve and CI groups (Fig. 5C). Because we included only axons with at least two boutons contained in our sample volume (≈6 × 10 × 12 μm), this frequency is almost certainly higher than the actual frequency over entire axons.

To assess the degree of similarity in synaptic connectivity between boutons on an axon, we compared each bouton to each of its neighbors by dividing the larger PSD area by the smaller. The average ratio of PSD areas between boutons in the naïve group was 2.5 ± 0.4, and was significantly larger at 4.1 ± 0.5 in the FC group (Fig. 5D). There was no correlation between the PSD ratio of bouton pairs and the distance between them in any of the groups (Fig. 5E). To determine whether the distribution of PSD sizes on axons was random, we shuffled the bouton pairs within each rat. PSD ratios from five iterations of random bouton pairings were averaged and compared to the real pairs. The PSD ratios in the naïve and CI groups
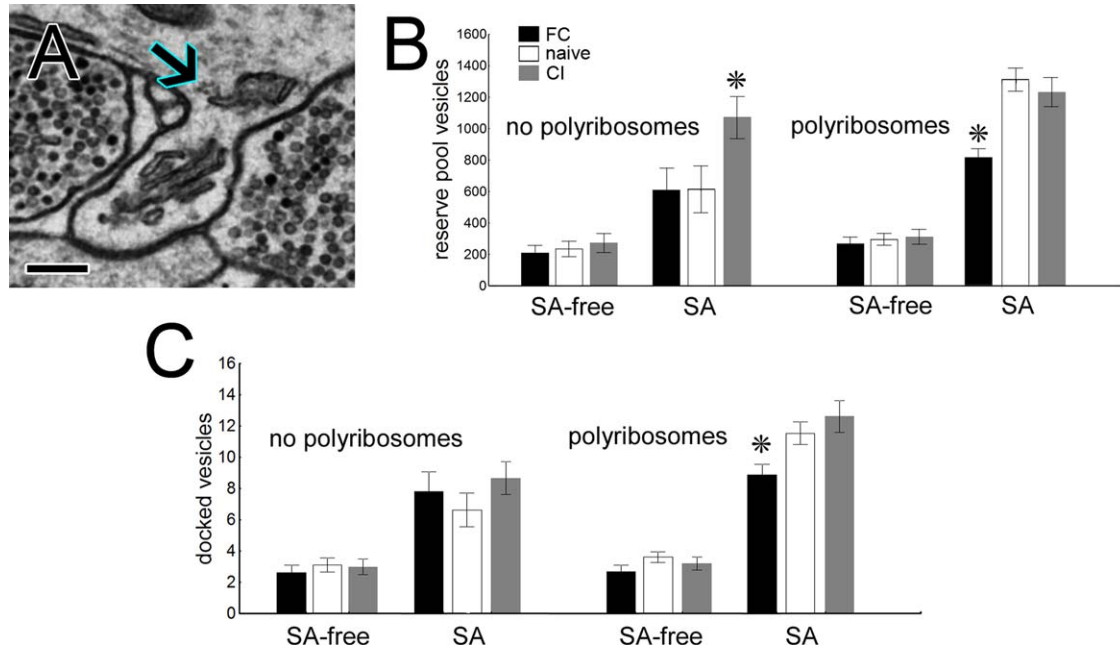
Figure 4. Polyribosomes differentiate boutons and synapses. **A:** Polyribosome (arrow) at the base of a spine containing a spine apparatus. **B:** The reserve pool is larger in the CI group in boutons presynaptic to spines with a spine apparatus without polyribosomes, and smaller in the FC group in boutons presynaptic to spines with a spine apparatus and polyribosomes (*$P < 0.03$). The reserve pool of boutons presynaptic to a spine apparatus was larger when polyribosomes were present in the naïve group ($P < 0.0001$). **C:** The number of docked vesicles at synapses is lower in the FC group when both a spine apparatus and polyribosomes are present in the postsynaptic spine (*$P > 0.01$). Scale bar = 250 nm. [Color figure can be viewed in the online issue, which is available at wileyonlinelibrary.com.]

were significantly different from the ratios between randomly paired boutons, with the naïve ratio increasing to 3.5 ± 0.4 and the CI ratio increasing from 2.8 ± 0.3 to 4.0 ± 0.3. The ratios in the FC group were not different from the random ratios (Fig. 5F). The highest observed ratio in the naïve group was 8.9, while in the FC group the maximum was 29.1. The maximum after shuffling in the naïve group went up to 24.5, while in the FC group it remained at 29.1. This demonstrates that there is a degree of coherence in synaptic connectivity between boutons, and this coherence is presumably lost when some PSDs enlarge with FC training and others do not. PSD enlargement with FC thus may not occur at all boutons along particular axons, but at individual synapses.

Synapse number varies between boutons and training groups

Individual synapses were defined as instances of synaptic contact between a single bouton and a single dendritic spine or shaft. Cases in which the PSD on a single spine was segmented were considered single synapses. Hippocampal boutons are well known to form synapses with more than one dendritic spine, and the frequency of multiple-synapse boutons (MSBs) has been observed to increase under certain conditions (Sorra and Harris, 1993; Harris, 1995; Woolley et al., 1996; Toni et al.,

1999; Yankova et al., 2001; Geinisman et al., 2001; Fiala et al., 2002). In the naïve group, 16% of boutons on axon segments formed synapses with more than one dendritic spine or shaft (Fig. 6A,B). The percentage of MSBs on the axon segments was not significantly different between training groups, although the mean was nonsignificantly higher in the FC group (Fig. 6C). Dendritic shaft synapses were formed by 6% of boutons, and of these half were on single-synapse boutons and half were on MSBs with a spine synapse. All boutons forming shaft synapses were on axons with at least one bouton forming a spine synapse (i.e., no axons were found which exclusively formed shaft synapses). In addition, 3% of boutons on the naïve axon segments did not have any postsynaptic partners. Each of these nonsynaptic boutons was found on an axon with at least one other bouton forming a spine synapse. The percentage of nonsynaptic boutons was significantly greater at 12% in the FC group (Fig. 6D). Reflecting the combined increase in MSBs and nonsynaptic boutons, the percentage of single-synapse boutons was significantly lower in the FC group (Fig. 6D). Given that the distance between boutons was equal between the FC and naïve groups (Fig. 5C), this suggests rearrangement of spine synapses from some boutons onto others.

Of the MSBs formed on the reconstructed dendrites, 10% formed multiple synapses onto different spines from
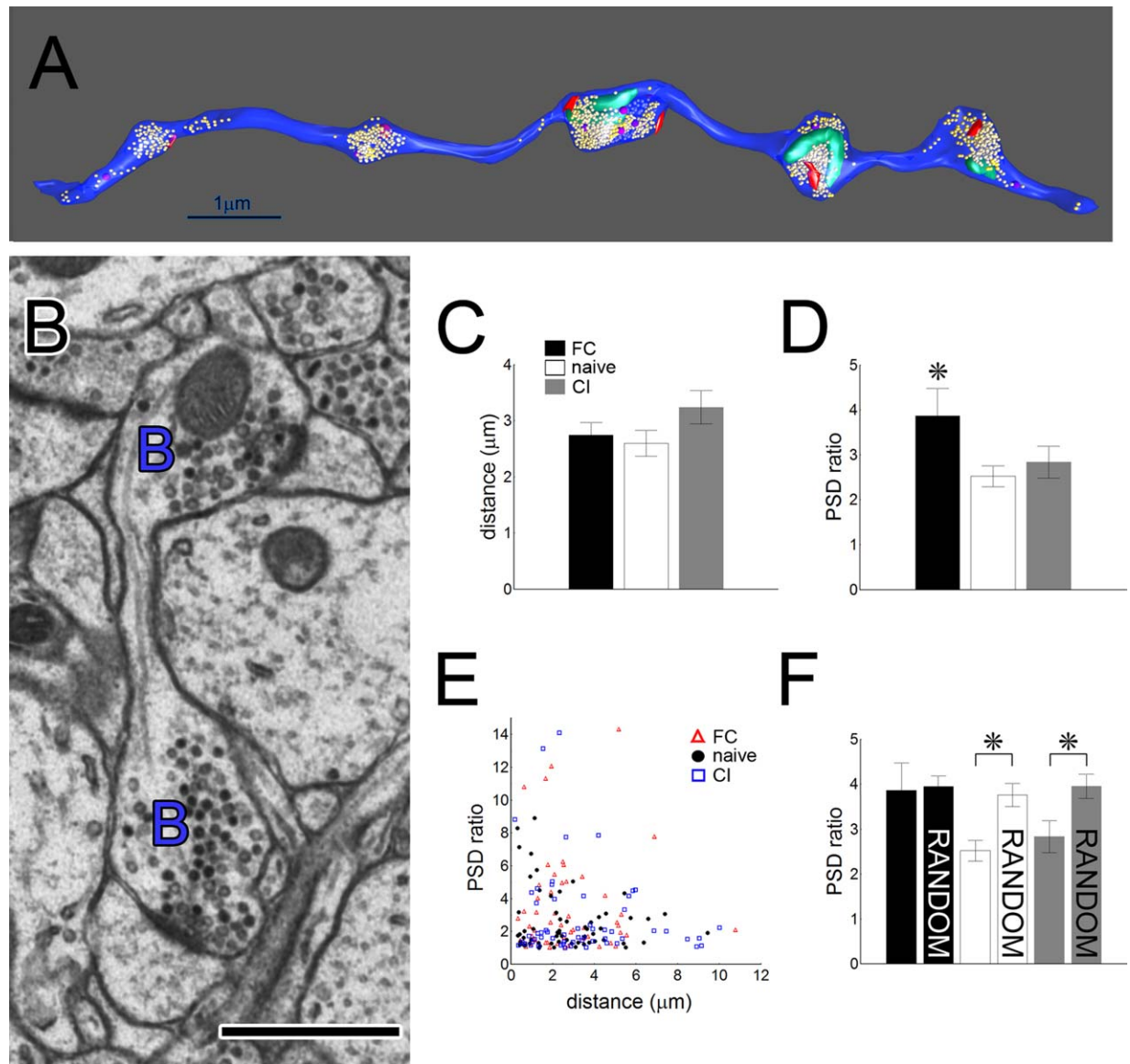
Figure 5. Boutons along an axon are similar. **A:** Reconstructed axon segment from a fear-conditioned rat showing five boutons with vesicles (yellow), PSDs (red), mitochondria (green), and small dense-core vesicles (pink). **B:** Electron micrograph showing two consecutive boutons (B) on an axon. **C:** Learning did not alter the distance between boutons on an axon ($P = 0.23$). **D:** The ratio of PSD areas on neighboring boutons increased with fear conditioning. FC $n = 77$, naïve $n = 68$, CI $n = 65$ (*$P < 0.05$). **E:** The ratio of PSD areas on neighboring boutons is not correlated with the distance between them. **F:** Comparison of the ratio of PSD areas on neighboring boutons with ratios of randomly shuffled PSDs. The ratios in the naïve and conditioned inhibition groups are significantly nonrandom (*$P < 0.05$). Legend in A applies throughout. Scale bar = 1 μm in B.

the same dendrite in the naïve group (7 of 58 in the naïve group, 9 of 93 in the FC group, and 2 of 42 in the CI group). Only one of these involved two branches of a branched spine, and in all cases mature axons and/or dendrites ran between the spines or branches. This is in agreement with previous observations and again confirms that same-dendrite MSBs do not result from "spine splitting" (Sorra and Harris, 1993; Toni et al., 1999; Fiala et al., 2002). Of the MSBs in the whole dataset, 10% carried three synapses and another 2% carried four (25 and

5 of 249, respectively), which was too few for meaningful analysis. The size of the reserve vesicle pool scaled roughly linearly with the number of synapses, as did the total PSD area on each bouton (Fig. 6F,G). There were no effects of training on these measures, so the groups were pooled for analysis.

Boutons with two synapses had approximately twice as much PSD area as boutons with one synapse (Fig. 6G). There was also no difference in PSD area between individual synapses on two-synapse MSBs and single-synapse

boutons (MSB: 0.061 ± 0.004, $n = 434$; single: 0.065 ± 0.003 μm^2, $n = 929$, $P = 0.47$). This indicates that boutons do not carry a single synapse worth of PSD, divided across one or more synapses. Rather, boutons scale up to support multiple full-sized synapses. Because this could be due to uniformity among MSBs or to some MSBs having multiple large PSDs and some having multiple small PSDs, the size relationships between PSDs on the same two-synapse MSB were examined. We compared the smaller and larger PSD of each pair with the smaller and larger halves of the single synapse population, divided by the median within each individual rat. There was no difference in PSD area between the MSB synapses and the single synapses, nor were the overall distributions different (Fig. 6H,I). To directly assess the similarity between PSDs on a bouton, we divided the larger of two PSDs on an MSB by the smaller. This ratio was equivalent to the one obtained by randomly shuffling the MSB PSDs within each rat (Fig. 6J). Predictably, the areas of the larger and smaller PSD were correlated if both or neither were associated with a spine apparatus, but not if only one was (Fig. 6K). All told, these results indicate that individual synapses on MSBs are no different from synapses on single synapse boutons, and have no particular size relationship to each other.

Mitochondria and small dense-core vesicles occur in boutons with large PSDs

Mitochondria are plentiful in axons and almost always occur in boutons, appearing very rarely along thin axon shafts (Fig. 7A). In the naïve group 35% of boutons contained at least one mitochondrion; this percentage was unaffected by training (Fig. 7B). PSD area on boutons with mitochondria was significantly greater than on boutons lacking mitochondria, and boutons with mitochondria in the FC group had even larger PSDs than those in the naïve group (Fig. 7C).

Large dense-core vesicles (90–120 nm) in axons contain neuropeptides and possibly amine neurotransmitters; axons containing these vesicles were very rare in our material and were excluded from the dataset. Small dense-core vesicles (sDCVs), in contrast, are ≈80 nm in diameter and are found in the reserve pool of asymmetric axons, not near the active zone (Fig. 8A). In immature neurons these vesicles have been shown traffic active zone proteins from the soma, sometimes appearing in aggregates (Zhai et al., 2001; Shapira et al., 2003; Tao-Cheng, 2007). In mature hippocampus, sDCVs appear more frequently in boutons after slice preparation, suggesting upregulation during a period of synaptic disruption and synaptogenesis (Fiala et al., 2003; Sorra et al., 2006).

Proteins essential for building the presynaptic active zone are carried on sDCVs, so their presence represents the potential for active zone enlargement or addition, and depletion would be expected in boutons that have recently enlarged (Sorra et al., 2006). In our material sDCVs occur in 38% of naïve boutons, and this percentage was significantly higher at 46% in the FC group (Fig. 8B). There were an average of 3.6 ± 0.2 DCVs in boutons that had them, and this number was smaller at 2.5 ± 0.3 in the CI group ($P < 0.01$) but was 3.2 ± 0.2 in the FC group, which was not different from naïve. Synapses with a spine apparatus were more likely to have presynaptic sDCVs than those without (63% vs. 33%, respectively).

To determine the relationship between synapse parameters and sDCVs, we examined synapses on single-synapse boutons. PSD area was greater on boutons containing sDCVs, but was smaller in the CI group on these boutons (Fig. 8C). This is somewhat surprising given that smaller synapses in theory have more room to enlarge and might be expected to have more sDCVs, but it is also possible that more sDCVs are necessary to facilitate turnover of proteins at large active zones. Synapses with a spine apparatus had significantly more docked and reserve pool vesicles per sDCV (Fig. 8D,E). This could signify either a greater potential for active zone enlargement at smaller synapses, or depletion of sDCVs due to recent enlargement of larger synapses. The ratios of docked and reserve pool vesicles to sDCVs ratios were also smaller in the FC group at synapses with a spine apparatus (Fig. 8D,E). This does not reflect a difference in the number of sDCVs per synapse, but rather the smaller number of vesicles at these boutons in the FC group.

The smaller vesicle pools seen in the FC group were specific to synapses with both a spine apparatus and polyribosomes (Fig. 4). We therefore examined these particular synapses with respect to sDCVs. The number of vesicles in both pools was larger in boutons with sDCVs, and the smaller pools in the FC group were specific to boutons with sDCVs (Fig. 8F,G). (There was, however, a nonsignificantly larger number of vesicles in the CI group when sDCVs were present, and nonsignificantly smaller number in the FC group in the absence of sDCVs.) A potential explanation is that sDCVs are delivered to boutons with actively enlarging synapses but are incorporated into the active zone on a longer time scale.

The presumed rearrangement of single-synapse boutons into MSBs and nonsynaptic boutons between the naïve and FC groups suggests that new synapses were formed at MSBs. Since sDCVs are likely involved in synaptogenesis, we examined MSBs with respect to sDCVs. The percentage of MSBs with sDCVs was higher in the FC group than in the naïve group, while there was no significant difference between MSBs and single-synapse

boutons in the naïve or CI groups (Fig. 8H). This could be accounted for by the delivery of sDCVs to boutons that are actively adding synapses. The number of docked and reserve pool vesicles and PSD area per sDCV were larger on MSBs, again suggesting either lower potential for add-

ing active zone or recent depletion of sDCVs (Fig. 8I–K). The ratio of reserve pool vesicles to sDCVs was lower on single synapses in the FC group, and there was a non-significant difference in this direction on MSBs as well (Fig. 8J). This is consistent with delivery of sDCVs to
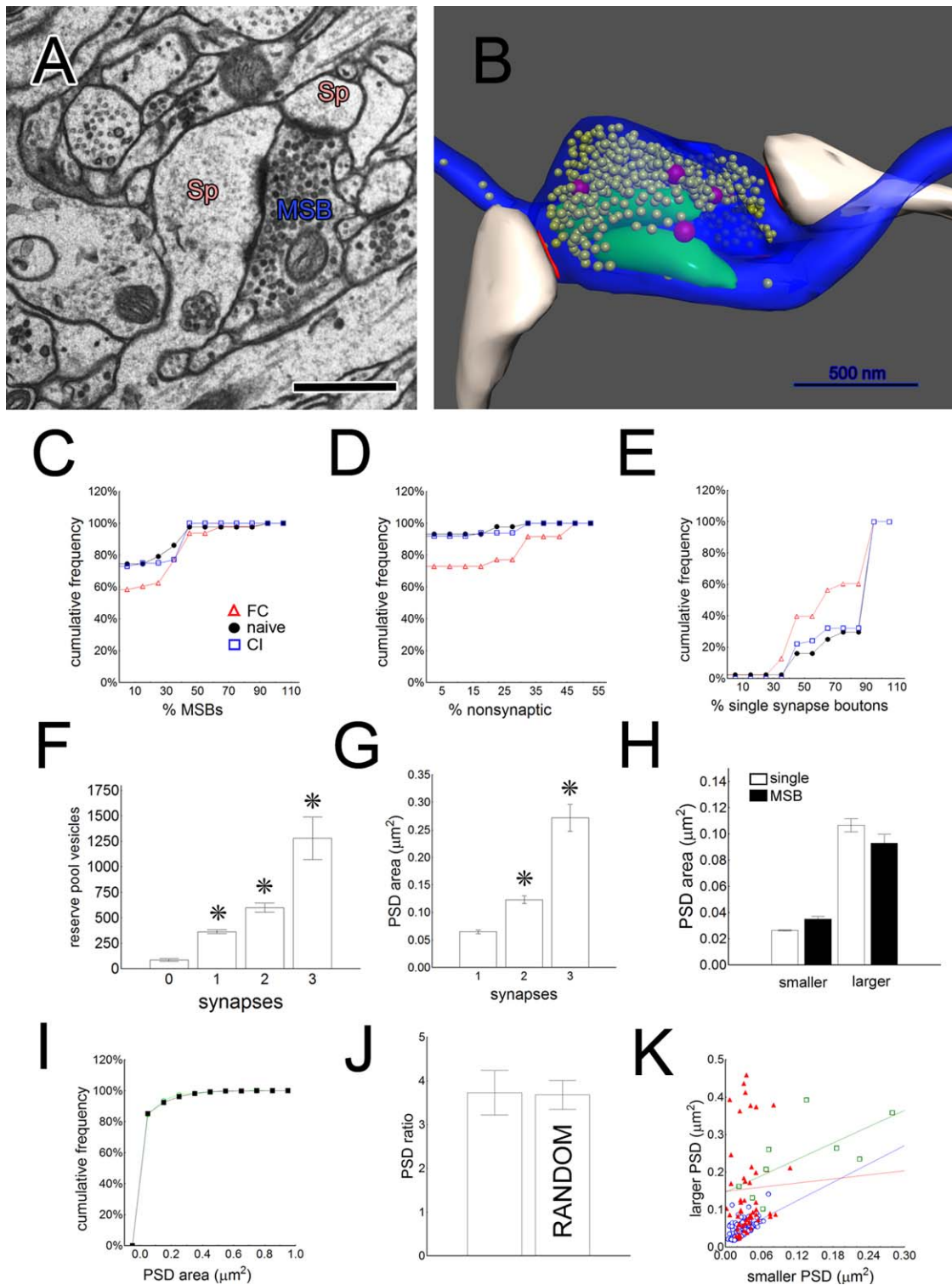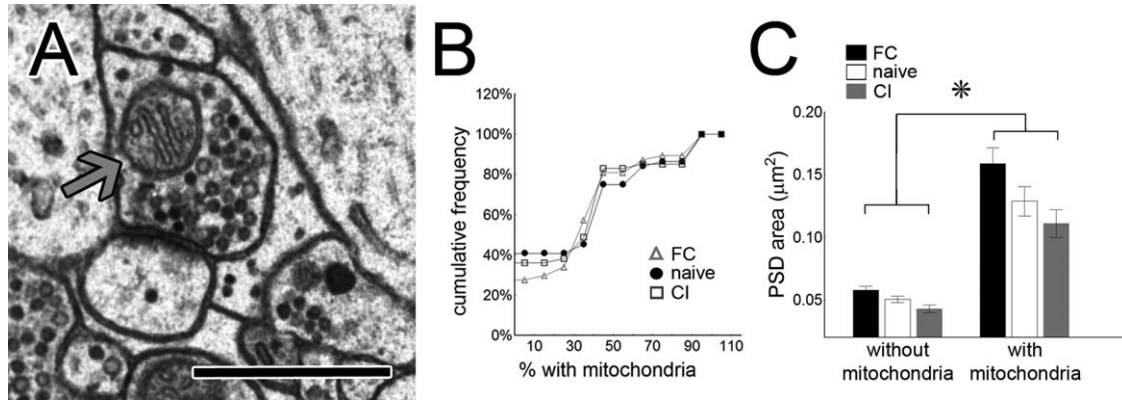

Figure 6

Figure 7. Mitochondria in boutons. **A:** Electron micrograph of a bouton containing a cross-sectioned mitochondrion (arrow). **B:** Frequency histogram of the percentage of boutons on each axon that contain mitochondria. Training groups were not significantly different. FC $n = 48$, naïve $n = 44$, CI $n = 50$ (Kruskal–Wallis ANOVA by ranks, $P = 0.39$). **C:** Boutons with mitochondria have larger PSDs than boutons without. No mitochondria: FC $n = 303$, naïve $n = 262$, CI $n = 192$; mitochondria: FC $n = 180$, naïve $n = 145$, CI $n = 97$ (*$P < 0.01$). Scale bar = 500 nm.

smaller boutons whose synapses are enlarging faster than the associated reserve pool.

DISCUSSION

Our examination of the morphological features of LAd axons after learning revealed diversity in synaptic structure, even at the level of single boutons. We found that the relationship between the PSD and the docked vesicle pool is not entirely linear, and that during consolidation of fear conditioning the relationship between presynaptic and postsynaptic morphology is altered. These observations together suggest that presynaptic and postsynaptic changes might occur on different time scales, and also raise the possibility that synapses exhibit functionally distinct configurations of presynaptic and postsynaptic elements, perhaps reflecting experience. We found also that in naïve and conditioned inhibition animals neighboring boutons on an axon are similar to each other in PSD area,

but that fear-conditioned animals show a random distribution of PSD areas, presumably due to changes in individual boutons and not along entire axons. Multiple-synapse boutons in our material carried individual synapses similar to those on single-synapse boutons, and we found rearrangement of the number of synapses on boutons between the naïve and fear-conditioned groups. Overall, we observed a number of structural changes in boutons and axons suggestive of morphological changes and reorganization during consolidation of learning.

Morphological correlates of synapse strength vary independently

The efficacy of a synapse is determined by the presynaptic release probability (P_r), the number of release sites (N), and the magnitude of the postsynaptic response (q) when release occurs (del Castillo and Katz, 1954; Zucker, 1989). While little is known about LA ultrastructure, the

Figure 6. Boutons support multiple synapses. **A:** Electron micrograph of a MSB forming synapses with two different spines (Sp). **B:** Reconstruction of an MSB (blue) contacting two dendritic spines (gray) showing vesicles (yellow), PSDs (red), mitochondria (green), and small dense-core vesicles (pink). **C:** Frequency histogram of the percentage of boutons on each axon segment which are MSBs. Training groups were not significantly different. FC $n = 48$, naïve $n = 44$, CI $n = 50$ (Kruskal–Wallis ANOVA by ranks, $P = 0.18$). **D:** The percentage of boutons on each axon which are nonsynaptic was higher in the FC group. (Kruskal–Wallis ANOVA by ranks, $P < 0.005$). **E:** The percentage of single-synapse boutons on each axon was lower in the FC group (Kruskal–Wallis ANOVA by ranks, $P < 0.003$). **F:** The reserve pool scales with synapse number. Each group is significantly different from all of the others. 0 $n = 21$, 1 $n = 734$, 2 $n = 180$, 3 $n = 22$ (*$P < 0.001$). **G:** Total bouton PSD area scales with synapse number. Each group is significantly different from all of the others. 1 $n = 930$, 2 $n = 215$, 3 $n = 24$ (*$P < 0.001$). **H:** On boutons with two synapses ($n = 216$), the larger and smaller of the two PSDs are equal in size to the average of the larger and smaller halves of the single-synapse population ($n = 930$), respectively. **I:** The distributions of individual PSD areas on single synapse boutons (green) and MSBs are equal. **J:** The ratio of the larger to the smaller of two PSDs on the same bouton is equal to a random shuffle of the PSDs. **K:** The larger and smaller PSDs on an MSB are correlated if both (green squares, $R^2 = 0.45$, $n = 9$) or neither (blue circles, $R^2 = 0.28$, $n = 112$) are associated with a spine apparatus, but not if only one is (red triangles, $R^2 = 0.0007$, $n = 53$). Scale bar = 500 nm in A.
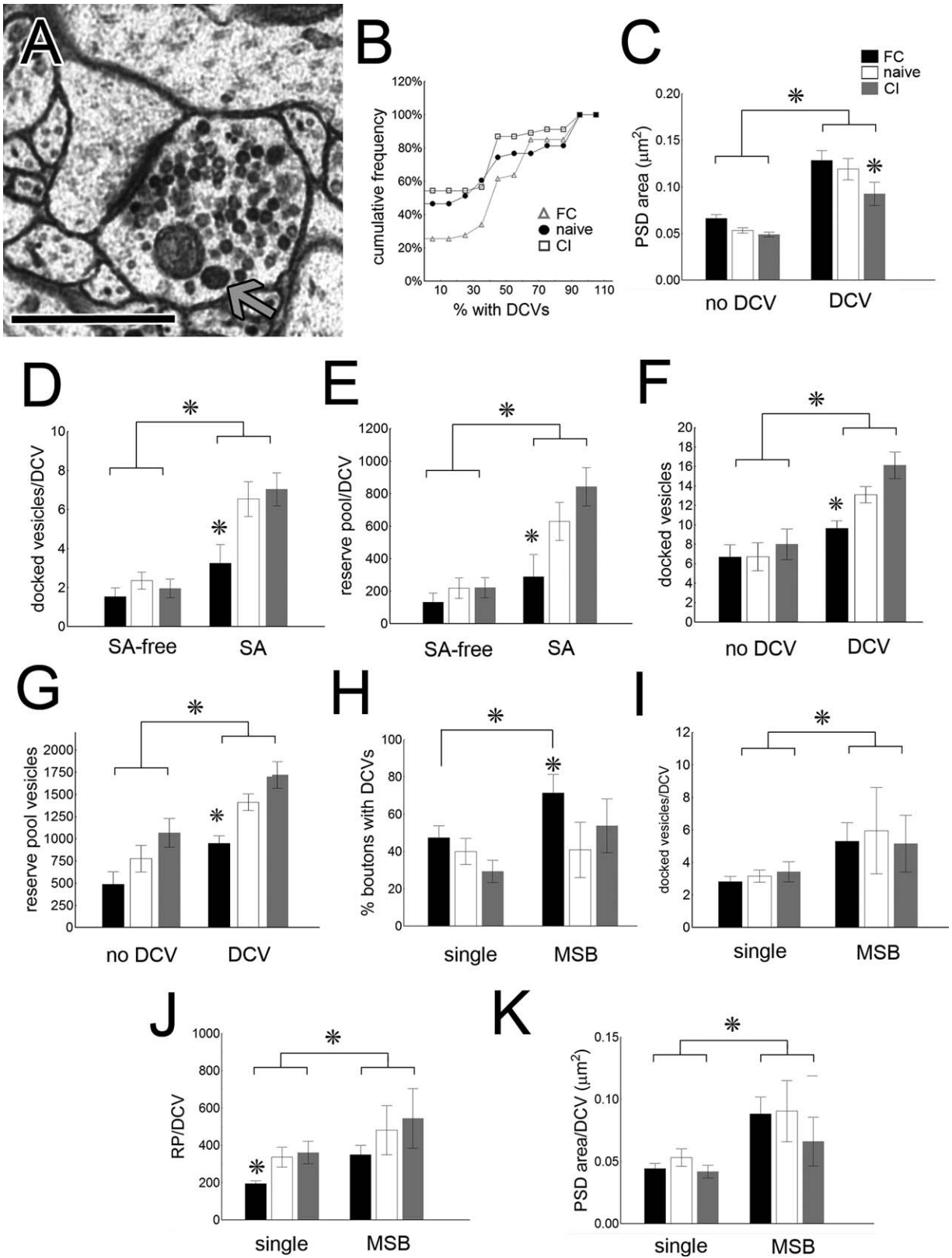
Figure 8

synaptic morphology of at least one forebrain area, CA1 of hippocampus, has been better studied with respect to function. The number of docked vesicles in hippocampal cultures is equal to the size of the readily releasable pool, which in turn is directly proportional to P_r (Dobrunz and Stevens, 1997; Murthy et al., 2001; Schikorski and Stevens, 2001; Dobrunz, 2002). On the postsynaptic side, the size of the PSD is proportional to both the total number of ionotropic glutamate receptors and the AMPA to NMDA receptor ratio (Takumi et al., 1999; Ganeshina et al., 2004a,b). Docked vesicle number and PSD area could therefore represent P_r and possibly q at these synapses. There is a tight linear correlation between docked vesicle number and PSD area in hippocampus (Schikorski and Stevens, 1997). Curiously, though, there is no relationship between P_r and either the amplitude of the postsynaptic response or the amount of GluR2 receptor subunits at individual synapses under baseline conditions (Dobrunz and Stevens, 1997; Tokuoka and Goda, 2008). This could be an artifact of the immature developmental stage of the preparations used in these experiments, but it demonstrates the potential uncoupling of P_r and q at single synapses.

We found a significant correlation between PSD area and docked vesicle number in LA, as in hippocampus (Harris and Sultan, 1995; Schikorski and Stevens, 1997). This relationship was not entirely linear, however. Our larger morphological synapse type, defined by the presence of a spine apparatus, had a significantly higher ratio of PSD to docked vesicles. One potential explanation for this is that expanding the readily releasable pool provides diminishing returns as P_r approaches saturation. Increasing synapse strength when P_r is already high may be better effected by adding postsynaptic receptors, which would explain the bias towards more PSD at the largest synapses. On the other hand, limiting P_r could be one mechanism for reigning in synapse strength at the upper end of the range. It is also possible that there are discrete configurations of presynaptic and postsynaptic machinery, potentially with functional distinctions. The molecular composition of LA synapses is unknown, but if all of the molecules do not scale proportionally the PSD could be very different between synapses. This would allow the possibility of a more discrete relationship between the pre- and postsynaptic elements; for example, the ratio of docked vesicles to AMPA receptors could be constant among all synapses.

Morphology of synapses during consolidation of fear learning

Excitatory synaptic responses are increased in the LA after fear conditioning, implying an increase in at least one if not more of these parameters (McKernan and Shinnick-Gallagher, 1997; Rogan et al., 1997). Indeed, P_r has been reported to be higher in LA slices made from fear-conditioned rats 24 hours after conditioning (McKernan and Shinnick-Gallagher, 1997; Tsvetkov et al., 2002; Zinebi et al., 2002, 2003; Schroeder and Shinnick-Gallagher, 2005). Glutamate receptors are also added to LA synapses with fear conditioning, and fear conditioning involves a number of presumably postsynaptic molecular mechanisms (Rodrigues et al., 2004; Maren, 2005; Rumpel et al., 2005; Yeh et al., 2006). Both P_r and q thus appear to increase at the population level. There are unfortunately no data on P_r and conditioned inhibition.

Changes in synaptic response are evident immediately after fear conditioning, while changes in P_r have only been assessed after consolidation. Our observation of higher PSD area on boutons in our fear conditioning certainly supports an immediate increase in q. We did not, however, observe a significant difference in docked vesicle number in the overall population in our training groups. If docked vesicles do reflect P_r in the LA, multiple explanations for the discrepancy between our data and

Figure 8. **A:** A small dense core vesicle (arrow) in a bouton. **B:** Frequency histogram of the percentage of boutons on each axon that contain dense-core vesicles. The percentage was higher in the FC group. FC $n = 48$, naïve $n = 44$, CI $n = 50$ (Kruskal–Wallis ANOVA by ranks, $P < 0.02$). **C:** Boutons with small dense-core vesicles (sDCVs) have larger PSDs than boutons without. No sDCVs: FC $n = 256$, naïve $n = 245$, CI $n = 184$; sDCVs: FC $n = 215$, naïve $n = 151$, CI $n = 89$ (*$P < 0.05$). **D:** There are more docked vesicles per sDCV in boutons presynaptic to a spine apparatus, and this ratio is higher in the FC group than the naïve at these synapses (*$P < 0.005$). **E:** The ratio of reserve pool vesicles to sDCVs is larger on boutons presynaptic to a spine apparatus, but is smaller on these spines in the FC group. SA-free: FC $n = 111$, naïve $n = 71$, CI $n = 48$; SA: FC $n = 60$, naïve $n = 32$, CI $n = 21$ (*$P < 0.001$). **F:** At synapses with both a spine apparatus and polyribosomes, there are more docked vesicles at synapses with sDCVs, and fewer docked vesicles at synapses with sDCVs in the FC group (*$P < 0.01$). **G:** At synapses with both a spine apparatus and polyribosomes, there are more reserve pool vesicles at synapses with sDCVs, and fewer reserve pool vesicles at synapses with sDCVs in the FC group (*$P < 0.001$). **H:** The percentage of multiple-synapse boutons that contain sDCVs is higher in the FC group than the naïve, and in the FC group this percentage is higher between single- and multiple-synapse boutons. FC $n = 48$, naïve $n = 44$, CI $n = 50$ (*$P < 0.05$). **I:** The number of docked vesicles per sDCV is higher on MSBs (*$P < 0.001$). **J:** The ratio of reserve pool vesicles to sDCV number is greater on multiple-synapse boutons (**$P < 0.04$), and is smaller on single-synapse boutons with FC (*$P < 0.02$). MSBs: FC $n = 53$, naïve $n = 24$, CI $n = 15$; single synapse boutons: FC $n = 125$, naïve $n = 87$, CI $n = 56$. **K)** The ratio of PSD area to sDCVs is larger on MSBs (*$P < 0.002$). Scale bar = 500 nm.

the slice data are possible. The simplest explanation is that the observed changes occur slowly. Another possibility is that the increase in P_r observed in fear conditioning could be accounted for by changes in other factors influencing P_r such as Ca^{2+} buffering and Ca^{2+} responsiveness of vesicles (Sudhof, 2004). Although the overall average number of docked vesicles was constant between our naïve and fear-conditioned groups, we did find both more docked vesicles at synapses with a spine apparatus. There were more spines with a spine apparatus in the fear-conditioned group, but in addition there was a nonsignificantly larger number of spines without a spine apparatus (Ostroff et al., 2010). These are four times as numerous and their smaller number of docked vesicles swamped the average. However, their disproportionately smaller PSD area and the possibility that they are postsynaptically silent could mean that the larger synapses swamped the physiological response averages. The addition of synapses with larger PSDs and more docked vesicles would then be detected physiologically but not morphologically.

Morphology of boutons during consolidation of fear learning

Assuming that synapse enlargement is a primary event following fear conditioning, enlargement of any or all of PSD area, docked vesicle number, and reserve pool size would be expected. The difference in PSD size in our trained groups resulted in alterations in the relationship of the PSD to the vesicle pools. This could reflect learning-related changes in the basic composition of synapses, or a transient mismatch between synapse components that change on different time scales.

The primary postsynaptic morphological change in the fear-conditioned group is the addition of spines with a spine apparatus, which accounts for the increase in PSD area (Ostroff et al., 2010). This is presumably due to enlargement and acquisition of a spine apparatus by small synapses, although the possibility of spinogenesis creating these spines cannot be ruled out. Polyribosomes are up-regulated in the dendrites in the fear-conditioned group, and it is reasonable to postulate that their presence in an LA spine reflects either recent activity or recent plasticity given the requirement for translation during consolidation of fear conditioning (Helmstetter et al., 2008; Ostroff et al., 2010). PSD area at synapses on spines containing both a spine apparatus and polyribosomes is equal between the naïve and fear-conditioned groups (Ostroff et al., 2010). On the presynaptic side, we found that at these particular synapses both the reserve and docked vesicle pools were smaller in the fear-conditioned group specifically at boutons which contained sDCVs.

A number of explanations are possible for these observations, and we propose the simplest. PSD enlargement and addition of the spine apparatus may occur quickly after training and involve local protein synthesis at the synapse. Delivery of sDCVs to active or plastic boutons could also occur quickly, but enlargement of the active zone and reserve pool is achieved more slowly. The failure of docked vesicles to track the PSD is unlikely to be due to slow vesicle docking, as this can occur in seconds to minutes in hippocampus (Stevens and Tsujimoto, 1995; Stevens and Wesseling, 1998; Murthy and Stevens, 1999). Given the buildup of sDCVs relative to synaptic vesicles, failure to enlarge the active zone seems more likely. In that case, the extra sDCVs could later be used to enlarge the active zone, ultimately normalizing the ratio of docked vesicles to sDCVs. It is interesting that sDCVs build up in boutons in the fear-conditioned group, perhaps waiting to insert into the active zone. An intriguing possibility is that exocytosis of sDCVs is triggered by events that occur during consolidation as opposed to during training, perhaps via retrograde signaling from the postsynaptic side. This could also explain the failure of the reserve pool to scale up immediately.

Rearrangement of synapse distribution

We found no difference in the distance between boutons along axons between training groups, while we did see a lower number of single-synapse boutons in favor of MSBs and nonsynaptic boutons in the fear-conditioned group. This suggests rearrangement of synapses away from some boutons and onto others, although it does not exclude the possibility of some nonsynaptic boutons being newly formed. We found more MSBs containing sDCVs in the fear-conditioned group. There was a buildup of sDCVs in the single-synapse boutons that are most likely to be enlarging in the fear-conditioned group; by extension this could mean that the MSBs in the fear-conditioned group are also building synapses.

Synapses along axons and even within boutons are structurally independent

We found that neighboring boutons on the same axon tended to have similar amounts of PSD in naïve animals, but that this similarity vanished with fear conditioning. This was presumably because enlargement of some PSDs with fear conditioning does not occur uniformly along particular axons, but at individual synapses instead. Individual presynaptic neurons and axons in forebrain are known to form synapses with quite different properties, especially when the postsynaptic targets are different cell types (Rosenmund et al., 1993; Reyes et al., 1998; Koester and Johnston, 2005; Pelkey and McBain, 2007;

Branco et al., 2008). Neighboring boutons on cultured hippocampal axons have similar P_r, and this is effected through activity in the postsynaptic dendrite (Murthy et al., 1997; Branco et al., 2008). Nearby boutons on an axon experience the same pattern of action potentials, and this may be the source of coordinated P_r in the absence of salient activity in the dendrites. Coordinated, synapse-specific presynaptic and postsynaptic activity are believed to underlie synaptic changes during fear conditioning (LeDoux, 2000; Blair et al., 2001). Since neighboring boutons generally do not synapse on the same dendrite, they would not be under the same postsynaptic influence and would not alter equally unless their postsynaptic targets did. Our data indicate that synapse enlargement with fear conditioning is not driven only by presynaptic activity, but is specific to individual synapses.

Our results are consistent with the occurrence of synapse-specific changes in both P_r and q during fear conditioning. An important caveat is that nothing is known of the functional correlates of morphological features of LA synapses (or of nondevelopmental hippocampal synapses either, for that matter). We have certainly shown that structural changes occur on both sides of the synapse, and that these are individual to synapses, not to axons or dendrites. Another factor influencing the strength of synaptic transmission, N, is less easily observed. Because of our small tissue volume, we are not able to detect whether the number of synapses between individual axons and dendrites is changed with learning. We did observe the addition of boutons with no synapses, half of which contained sDCVs and were presumably able to construct an active zone. The addition of extra boutons could be a mechanism to bias connectivity toward particular axons, allowing the network to rewire via spine turnover (Chklovskii et al., 2004; De Roo et al., 2008; Xu et al., 2009; Yang et al., 2009). Boutons and vesicle pools are certainly motile and could turn over in the neuropil to facilitate activity-driven reorganization of synapses, allowing large-scale control over the number of release sites (De Paola et al., 2006; Gogolla et al., 2007; Becker et al., 2008; Staras et al., 2010). Storage of associative fear memories in the LA thus involves rearrangement of both presynaptic and postsynaptic elements, and possibly of connectivity.

Potential contribution of afferent origins

Another possible explanation involves the putative origin of the LA axons. The heaviest projections to LAd come from auditory thalamus and cortex, and the morphology of these is qualitatively indistinguishable on single EM sections (LeDoux et al., 1991a; Farb and LeDoux, 1997, 1999). Cortical afferents to LA display paired pulse facilitation, while thalamic afferents display paired pulse depression, suggesting that P_r is saturated at thalamic but not cortical synapses (Sigurdsson et al., 2010). In hippocampus, paired pulse facilitation is inversely correlated with P_r, with the synapses with the highest P_r showing the lowest facilitation or even depression (Dobrunz and Stevens, 1997; Murthy et al., 1997). It is likely, therefore, that cortical and thalamic projections do change differentially with learning, and tracer studies will be required to sort this out. There is also evidence in LA slices that spines postsynaptic to different fiber tracts differ markedly in size (Humeau et al., 2005). This raises the possibility that the spine apparatus is located in spines depending on the origin of the presynaptic partner. If true, our data would indeed reflect differential effects of learning on synapses from different areas. However, our data strongly discourage this interpretation. Boutons on the same axon and synapses on the same bouton are very different in size and their postsynaptic partners vary in their spine apparatus content. Although the synapse population is certainly not homogeneous in terms of afferent origin, there is no obvious morphological distinction between axons.

Our observations of axons and boutons reveal nuanced morphological relationships between the presynaptic and postsynaptic elements of synapses, and between boutons themselves. Overall, the results suggest that learning has morphological effects on individual synapses independent of their parent axon. An open question for the future is whether the differential effects of learning on presynaptic and postsynaptic structure are persistent or simply reflect different time courses of change.

ACKNOWLEDGMENTS

LITERATURE CITED

Alvarez VA, Sabatini BL. 2007. Anatomical and physiological plasticity of dendritic spines. Annu Rev Neurosci 30:79–97.

Barnes CA. 1995. Involvement of LTP in memory: are we "searching under the street light"? Neuron 15:751–754.

Barondes SH, Squire LR. 1972. Time and the biology of memory. Clin Neurosurg 19:381–396.

Becker N, Wierenga CJ, Fonseca R, Bonhoeffer T, Nagerl UV. 2008. LTD induction causes morphological changes of presynaptic boutons and reduces their contacts with spines. Neuron 60:590–597.

Bisaz R, Sandi C. 2010. The role of NCAM in auditory fear conditioning and its modulation by stress: a focus on the amygdala. Genes Brain Behav 9:353–364.

Blair HT, Schafe GE, Bauer EP, Rodrigues SM, LeDoux JE. 2001. Synaptic plasticity in the lateral amygdala: a cellular hypothesis of fear conditioning. Learn Mem 8:229–242.

Bourne J, Harris KM. 2007. Do thin spines learn to be mushroom spines that remember? Curr Opin Neurobiol 17:381–386.

Bourne JN, Harris KM. 2008. Balancing structure and function at hippocampal dendritic spines. Annu Rev Neurosci 31: 47–67.

Branco T, Staras K, Darcy KJ, Goda Y. 2008. Local dendritic activity sets release probability at hippocampal synapses. Neuron 59:475–485.

Chklovskii DB, Mel BW, Svoboda K. 2004. Cortical rewiring and information storage. Nature 431:782–788.

Davis HP, Squire LR. 1984. Protein synthesis and memory: a review. Psychol Bull 96:518–559.

De Paola V, Arber S, Caroni P. 2003. AMPA receptors regulate dynamic equilibrium of presynaptic terminals in mature hippocampal networks. Nat Neurosci 6:491–500.

De Paola V, Holtmaat A, Knott G, Song S, Wilbrecht L, Caroni P, Svoboda K. 2006. Cell type-specific structural plasticity of axonal branches and boutons in the adult neocortex. Neuron 49:861–875.

De Roo M, Klauser P, Garcia PM, Poglia L, Muller D. 2008. Spine dynamics and synapse remodeling during LTP and memory processes. Prog Brain Res 169:199–207.

del Castillo J, Katz B. 1954. Quantal components of the end-plate potential. J Physiol 124:560–573.

Dobrunz LE. 2002. Release probability is regulated by the size of the readily releasable vesicle pool at excitatory synapses in hippocampus. Int J Dev Neurosci 20:225–236.

Dobrunz LE, Stevens CF. 1997. Heterogeneity of release probability, facilitation, and depletion at central synapses. Neuron 18:995–1008.

Fanselow MS, Poulos AM. 2005. The neuroscience of mammalian associative learning. Annu Rev Psychol 56:207–234.

Farb CR, LeDoux JE. 1997. NMDA and AMPA receptors in the lateral nucleus of the amygdala are postsynaptic to auditory thalamic afferents. Synapse 27:106–121.

Farb CR, Ledoux JE. 1999. Afferents from rat temporal cortex synapse on lateral amygdala neurons that express NMDA and AMPA receptors. Synapse 33:218–229.

Farb C, Aoki C, Milner T, Kaneko T, LeDoux J. 1992. Glutamate immunoreactive terminals in the lateral amygdaloid nucleus: a possible substrate for emotional memory. Brain Res 593:145–158.

Farb CR, Chang W, LeDoux JE. 2010. Ultrastructural characterization of noradrenergic- and beta-adrenergic receptor-containing profiles in the lateral nucleus of the amygdala. Front Behav Neurosci 4:162.

Fiala JC. 2005. Reconstruct: a free editor for serial section microscopy. J Microsc 218(Pt 1):52–61.

Fiala JC, Harris KM. 2001. Cylindrical diameters method for calibrating section thickness in serial electron microscopy. J Microsc 202(Pt 3):468–472.

Fiala JC, Allwardt B, Harris KM. 2002. Dendritic spines do not split during hippocampal LTP or maturation. Nat Neurosci 5:297–298.

Fiala JC, Kirov SA, Feinberg MD, Petrak LJ, George P, Goddard CA, Harris KM. 2003. Timing of neuronal and glial ultrastructure disruption during brain slice preparation and recovery in vitro. J Comp Neurol 465:90–103.

Gale GD, Anagnostaras SG, Godsil BP, Mitchell S, Nozawa T, Sage JR, Wiltgen B, Fanselow MS. 2004. Role of the basolateral amygdala in the storage of fear memories across the adult lifetime of rats. J Neurosci 24:3810–3815.

Ganeshina O, Berry RW, Petralia RS, Nicholson DA, Geinisman Y. 2004a. Differences in the expression of AMPA and NMDA receptors between axospinous perforated and nonperforated synapses are related to the configuration and size of postsynaptic densities. J Comp Neurol 468:86–95.

Ganeshina O, Berry RW, Petralia RS, Nicholson DA, Geinisman Y. 2004b. Synapses with a segmented, completely partitioned postsynaptic density express more AMPA receptors than other axospinous synaptic junctions. Neuroscience 125:615–623.

Geinisman Y, Berry RW, Disterhoft JF, Power JM, Van der Zee EA. 2001. Associative learning elicits the formation of multiple-synapse boutons. J Neurosci 21:5568–5573.

Gogolla N, Galimberti I, Caroni P. 2007. Structural plasticity of axon terminals in the adult. Curr Opin Neurobiol 17:516–524.

Gray EG. 1959a. Axo-somatic and axo-dendritic synapses of the cerebral cortex: an electron microscope study. J Anat 93:420–433.

Gray EG. 1959b. Electron microscopy of synaptic contacts on dendrite spines of the cerebral cortex. Nature 183:1592–1593.

Harris KM. 1995. How multiple-synapse boutons could preserve input specificity during an interneuronal spread of LTP. Trends Neurosci 18:365–369.

Harris KM, Sultan P. 1995. Variation in the number, location and size of synaptic vesicles provides an anatomical basis for the nonuniform probability of release at hippocampal CA1 synapses. Neuropharmacology 34:1387–1395.

Harris KM, Perry E, Bourne J, Feinberg M, Ostroff L, Hurlburt J. 2006. Uniform serial sectioning for transmission electron microscopy. J Neurosci 26:12101–12103.

Helmstetter FJ, Parsons RG, Gafford GM. 2008. Macromolecular synthesis, distributed synaptic plasticity, and fear conditioning. Neurobiol Learn Mem 89:324–337.

Hernandez PJ, Abel T. 2008. The role of protein synthesis in memory consolidation: progress amid decades of debate. Neurobiol Learn Mem 89:293–311.

Holtmaat A, Svoboda K. 2009. Experience-dependent structural synaptic plasticity in the mammalian brain. Nat Rev Neurosci 10:647–658.

Houser CR, Crawford GD, Salvaterra PM, Vaughn JE. 1985. Immunocytochemical localization of choline acetyltransferase in rat cerebral cortex: a study of cholinergic neurons and synapses. J Comp Neurol 234:17–34.

Humeau Y, Herry C, Kemp N, Shaban H, Fourcaudot E, Bissiere S, Luthi A. 2005. Dendritic spine heterogeneity determines afferent-specific Hebbian plasticity in the amygdala. Neuron 45:119–131.

Kasai H, Fukuda M, Watanabe S, Hayashi-Takagi A, Noguchi J. 2010. Structural dynamics of dendritic spines in memory and cognition. Trends Neurosci 33:121–129.

Klann E, Sweatt JD. 2008. Altered protein synthesis is a trigger for long-term memory formation. Neurobiol Learn Mem 89:247–259.

Koester HJ, Johnston D. 2005. Target cell-dependent normalization of transmitter release at neocortical synapses. Science 308:863–866.

Konur S, Yuste R. 2004. Imaging the motility of dendritic protrusions and axon terminals: roles in axon sampling and synaptic competition. Mol Cell Neurosci 27:427–440.

Kubota Y, Hatada SN, Kawaguchi Y. 2009. Important factors for the three-dimensional reconstruction of neuronal structures from serial ultrathin sections. Front Neural Circuits 3:4.

LeDoux JE. 2000. Emotion circuits in the brain. Annu Rev Neurosci 23:155–184.

LeDoux JE, Farb C, Ruggiero DA. 1990. Topographic organization of neurons in the acoustic thalamus that project to the amygdala. J Neurosci 10:1043–1054.

LeDoux JE, Farb CR, Milner TA. 1991a. Ultrastructure and synaptic associations of auditory thalamo-amygdala projections in the rat. Exp Brain Res 85:577–586.

LeDoux JE, Farb CR, Romanski LM. 1991b. Overlapping projections to the amygdala and striatum from auditory processing areas of the thalamus and cortex. Neurosci Lett 134:139–144.

Li R, Nishijo H, Wang Q, Uwano T, Tamura R, Ohtani O, Ono T. 2001. Light and electron microscopic study of cholinergic and noradrenergic elements in the basolateral nucleus

of the rat amygdala: evidence for interactions between the two systems. J Comp Neurol 439:411–425.

Lin H, Vicini S, Hsu FC, Doshi S, Takano H, Coulter DA, Lynch DR. 2010. Axonal alpha7 nicotinic ACh receptors modulate presynaptic NMDA receptor expression and structural plasticity of glutamatergic presynaptic boutons. Proc Natl Acad Sci U S A 107:16661–16666.

Maguschak KA, Ressler KJ. 2008. Beta-catenin is required for memory consolidation. Nat Neurosci 11:1319–1326.

Maren S. 2001. Neurobiology of Pavlovian fear conditioning. Annu Rev Neurosci 24:897–931.

Maren S. 2005. Synaptic mechanisms of associative memory in the amygdala. Neuron 47:783–786.

Marik SA, Yamahachi H, McManus JN, Szabo G, Gilbert CD. 2010. Axonal dynamics of excitatory and inhibitory neurons in somatosensory cortex. PLoS Biol 8:e1000395.

Mascagni F, McDonald AJ, Coleman JR. 1993. Corticoamygdaloid and corticocortical projections of the rat temporal cortex: a Phaseolus vulgaris leucoagglutinin study. Neuroscience 57: 697–715.

McDonald AJ. 1982. Neurons of the lateral and basolateral amygdaloid nuclei: a Golgi study in the rat. J Comp Neurol 212:293–312.

McDonald AJ. 1992. Projection neurons of the basolateral amygdala: a correlative Golgi and retrograde tract tracing study. Brain Res Bull 28:179–185.

McDonald AJ, Mascagni F. 1996. Cortico-cortical and cortico-amygdaloid projections of the rat occipital cortex: a Phaseolus vulgaris leucoagglutinin study. Neuroscience 71: 37–54.

McDonald AJ, Mascagni F. 1997. Projections of the lateral entorhinal cortex to the amygdala: a Phaseolus vulgaris leucoagglutinin study in the rat. Neuroscience 77:445–459.

McDonald AJ, Mascagni F. 2010. Neuronal localization of m1 muscarinic receptor immunoreactivity in the rat basolateral amygdala. Brain Struct Funct 215:37–48.

McDonald AJ, Pearson JC. 1989. Coexistence of GABA and peptide immunoreactivity in non-pyramidal neurons of the basolateral amygdala. Neurosci Lett 100:53–58.

McDonald AJ, Muller JF, Mascagni F. 2002. GABAergic innervation of alpha type II calcium/calmodulin-dependent protein kinase immunoreactive pyramidal neurons in the rat basolateral amygdala. J Comp Neurol 446:199–218.

McKernan MG, Shinnick-Gallagher P. 1997. Fear conditioning induces a lasting potentiation of synaptic currents in vitro. Nature 390:607.

Muller JF, Mascagni F, McDonald AJ. 2006. Pyramidal cells of the rat basolateral amygdala: synaptology and innervation by parvalbumin-immunoreactive interneurons. J Comp Neurol 494:635–650.

Muller JF, Mascagni F, McDonald AJ. 2007a. Postsynaptic targets of somatostatin-containing interneurons in the rat basolateral amygdala. J Comp Neurol 500:513–529.

Muller JF, Mascagni F, McDonald AJ. 2007b. Serotonin-immunoreactive axon terminals innervate pyramidal cells and interneurons in the rat basolateral amygdala. J Comp Neurol 505:314–335.

Muller JF, Mascagni F, McDonald AJ. 2009. Dopaminergic innervation of pyramidal cells in the rat basolateral amygdala. Brain Struct Funct 213:275–288.

Murthy VN, Stevens CF. 1999. Reversal of synaptic vesicle docking at central synapses. Nat Neurosci 2:503–507.

Murthy VN, Sejnowski TJ, Stevens CF. 1997. Heterogeneous release properties of visualized individual hippocampal synapses. Neuron 18:599–612.

Murthy VN, Schikorski T, Stevens CF, Zhu Y. 2001. Inactivity produces increases in neurotransmitter release and synapse size. Neuron 32:673–682.

Ostroff LE, Cain CK, Bedont J, Monfils MH, Ledoux JE. 2010. Fear and safety learning differentially affect synapse size and dendritic translation in the lateral amygdala. Proc Natl Acad Sci U S A 107:9418–9423.

Pelkey KA, McBain CJ. 2007. Differential regulation at functionally divergent release sites along a common axon. Curr Opin Neurobiol 17:366–373.

Phelps PE, Houser CR, Vaughn JE. 1985. Immunocytochemical localization of choline acetyltransferase within the rat neostriatum: a correlated light and electron microscopic study of cholinergic neurons and synapses. J Comp Neurol 238:286–307.

Pitkanen A, Savander V, LeDoux JE. 1997. Organization of intra-amygdaloid circuitries in the rat: an emerging framework for understanding functions of the amygdala. Trends Neurosci 20:517–523.

Pollak DD, Monje FJ, Zuckerman L, Denny CA, Drew MR, Kandel ER. 2008. An animal model of a behavioral intervention for depression. Neuron 60:149–161.

Quirk GJ, Repa JC, LeDoux JE. 1995. Fear conditioning enhances short-latency auditory responses of lateral amygdala neurons: Parallel recordings in the freely behaving rat. Neuron 15:1029–1039.

Rescorla RA. 1969. Conditioned inhibition of fear resulting from negative CS-US contingencies. J Comp Physiol Psychol 67:504–509.

Reyes A, Lujan R, Rozov A, Burnashev N, Somogyi P, Sakmann B. 1998. Target-cell-specific facilitation and depression in neocortical circuits. Nat Neurosci 1:279–285.

Rizzoli SO, Betz WJ. 2005. Synaptic vesicle pools. Nat Rev Neurosci 6:57–69.

Rodrigues SM, Schafe GE, LeDoux JE. 2004. Molecular mechanisms underlying emotional learning and memory in the lateral amygdala. Neuron 44:75–91.

Rogan MT, LeDoux JE. 1995. LTP is accompanied by commensurate enhancement of auditory-evoked responses in a fear conditioning circuit. Neuron 15:127.

Rogan MT, Staubli UV, LeDoux JE. 1997. Fear conditioning induces associative long-term potentiation in the amygdala. Nature 390:604.

Rogan MT, Leon KS, Perez DL, Kandel ER. 2005. Distinct neural signatures for safety and danger in the amygdala and striatum of the mouse. Neuron 46:309–320.

Rosenmund C, Stevens CF. 1996. Definition of the readily releasable pool of vesicles at hippocampal synapses. Neuron 16:1197–1207.

Rosenmund C, Clements JD, Westbrook GL. 1993. Nonuniform probability of glutamate release at a hippocampal synapse. Science 262:754–757.

Rumpel S, LeDoux J, Zador A, Malinow R. 2005. Postsynaptic receptor trafficking underlying a form of associative learning. Science 308:83–88.

Sah P, Westbrook RF, Luthi A. 2008. Fear conditioning and long-term potentiation in the amygdala: what really is the connection? Ann N Y Acad Sci 1129:88–95.

Schafe GE, LeDoux JE. 2000. Memory consolidation of auditory pavlovian fear conditioning requires protein synthesis and protein kinase A in the amygdala. J Neurosci 20:96RC.

Schafe GE, Nadel NV, Sullivan GM, Harris A, LeDoux JE. 1999. Memory consolidation for contextual and auditory fear conditioning is dependent on protein synthesis, PKA, and MAP kinase. Learn Mem 6:97–110.

Schafe GE, Atkins CM, Swank MW, Bauer EP, Sweatt JD, LeDoux JE. 2000. Activation of ERK/MAP kinase in the amygdala is required for memory consolidation of pavlovian fear conditioning. J Neurosci 20:8177–8187.

Schikorski T, Stevens CF. 1997. Quantitative ultrastructural analysis of hippocampal excitatory synapses. J Neurosci 17:5858–5867.

Schikorski T, Stevens CF. 2001. Morphological correlates of functionally defined synaptic vesicle populations. Nat Neurosci 4:391–395.

Schroeder BW, Shinnick-Gallagher P. 2005. Fear learning induces persistent facilitation of amygdala synaptic transmission. Eur J Neurosci 22:1775–1783.

Schweizer FE, Ryan TA. 2006. The synaptic vesicle: cycle of exocytosis and endocytosis. Curr Opin Neurobiol 16:298–304.

Seguela P, Wadiche J, Dineley-Miller K, Dani JA, Patrick JW. 1993. Molecular cloning, functional properties, and distribution of rat brain alpha 7: a nicotinic cation channel highly permeable to calcium. J Neurosci 13:596–604.

Shapira M, Zhai RG, Dresbach T, Bresler T, Torres VI, Gundelfinger ED, Ziv NE, Garner CC. 2003. Unitary assembly of presynaptic active zones from Piccolo-Bassoon transport vesicles. Neuron 38:237–252.

Shepherd GM, Harris KM. 1998. Three-dimensional structure and composition of CA3→CA1 axons in rat hippocampal slices: implications for presynaptic connectivity and compartmentalization. J Neurosci 18:8300–8310.

Shi CJ, Cassell MD. 1998a. Cascade projections from somatosensory cortex to the rat basolateral amygdala via the parietal insular cortex. J Comp Neurol 399:469–491.

Shi CJ, Cassell MD. 1998b. Cortical, thalamic, and amygdaloid connections of the anterior and posterior insular cortices. J Comp Neurol 399:440–468.

Shi CJ, Cassell MD. 1999. Perirhinal cortex projections to the amygdaloid complex and hippocampal formation in the rat. J Comp Neurol 406:299–328.

Sigurdsson T, Doyere V, Cain CK, LeDoux JE. 2007. Long-term potentiation in the amygdala: a cellular mechanism of fear learning and memory. Neuropharmacology 52:215–227.

Sigurdsson T, Cain CK, Doyere V, LeDoux JE. 2010. Asymmetries in long-term and short-term plasticity at thalamic and cortical inputs to the amygdala in vivo. Eur J Neurosci 31:250–262.

Sorra KE, Harris KM. 1993. Occurrence and three-dimensional structure of multiple synapses between individual radiatum axons and their target pyramidal cells in hippocampal area CA1. J Neurosci 13:3736–3748.

Sorra KE, Mishra A, Kirov SA, Harris KM. 2006. Dense core vesicles resemble active-zone transport vesicles and are diminished following synaptogenesis in mature hippocampal slices. Neuroscience 141:2097–2106.

Staras K, Branco T, Burden JJ, Pozo K, Darcy K, Marra V, Ratnayaka A, Goda Y. 2010. A vesicle superpool spans multiple presynaptic terminals in hippocampal neurons. Neuron 66:37–44.

Stettler DD, Yamahachi H, Li W, Denk W, Gilbert CD. 2006. Axons and synaptic boutons are highly dynamic in adult visual cortex. Neuron 49:877–887.

Stevens CF. 1998. A million dollar question: does LTP = memory? Neuron 20:1–2.

Stevens CF, Tsujimoto T. 1995. Estimates for the pool size of releasable quanta at a single central synapse and for the time required to refill the pool. Proc Natl Acad Sci U S A 92:846–849.

Stevens CF, Wesseling JF. 1998. Activity-dependent modulation of the rate at which synaptic vesicles become available to undergo exocytosis. Neuron 21:415–424.

Sudhof TC. 2004. The synaptic vesicle cycle. Annu Rev Neurosci 27:509–547.

Sutton MA, Schuman EM. 2006. Dendritic protein synthesis, synaptic plasticity, and memory. Cell 127:49–58.

Takumi Y, Ramirez-Leon V, Laake P, Rinvik E, Ottersen OP. 1999. Different modes of expression of AMPA and NMDA receptors in hippocampal synapses. Nat Neurosci 2:618–624.

Tao-Cheng JH. 2007. Ultrastructural localization of active zone and synaptic vesicle proteins in a preassembled multi-vesicle transport aggregate. Neuroscience 150:575–584.

Tokuoka H, Goda Y. 2008. Activity-dependent coordination of presynaptic release probability and postsynaptic GluR2 abundance at single synapses. Proc Natl Acad Sci U S A 105:14656–14661.

Toni N, Buchs PA, Nikonenko I, Bron CR, Muller D. 1999. LTP promotes formation of multiple spine synapses between a single axon terminal and a dendrite. Nature 402:421–425.

Tsvetkov E, Carlezon JWA, Benes FM, Kandel ER, Bolshakov VY. 2002. Fear conditioning occludes LTP-induced presynaptic enhancement of synaptic transmission in the cortical pathway to the lateral amygdala. Neuron 34:289.

Umeda T, Ebihara T, Okabe S. 2005. Simultaneous observation of stably associated presynaptic varicosities and postsynaptic spines: morphological alterations of CA3-CA1 synapses in hippocampal slice cultures. Mol Cell Neurosci 28:264–274.

Woolley CS, Wenzel HJ, Schwartzkroin PA. 1996. Estradiol increases the frequency of multiple synapse boutons in the hippocampal CA1 region of the adult female rat. J Comp Neurol 373:108–117.

Xu T, Yu X, Perlik AJ, Tobin WF, Zweig JA, Tennant K, Jones T, Zuo Y. 2009. Rapid formation and selective stabilization of synapses for enduring motor memories. Nature 462:915–919.

Yang G, Pan F, Gan WB. 2009. Stably maintained dendritic spines are associated with lifelong memories. Nature 462:920–924.

Yankova M, Hart SA, Woolley CS. 2001. Estrogen increases synaptic connectivity between single presynaptic inputs and multiple postsynaptic CA1 pyramidal cells: a serial electron-microscopic study. Proc Natl Acad Sci U S A 98:3525–3530.

Yeh SH, Mao SC, Lin HC, Gean PW. 2006. Synaptic expression of glutamate receptor after encoding of fear memory in the rat amygdala. Mol Pharmacol 69:299–308.

Zhai RG, Vardinon-Friedman H, Cases-Langhoff C, Becker B, Gundelfinger ED, Ziv NE, Garner CC. 2001. Assembling the presynaptic active zone: a characterization of an active one precursor vesicle. Neuron 29:131–143.

Zinebi F, McKernan M, Shinnick-Gallagher P. 2002. Expression of fear-conditioning is accompanied by increased paired-pulse depression within the amygdala. Pharmacol Biochem Behav 71:393–400.

Zinebi F, Xie J, Liu J, Russell RT, Gallagher JP, McKernan MG, Shinnick-Gallagher P. 2003. NMDA currents and receptor protein are downregulated in the amygdala during maintenance of fear memory. J Neurosci 23:10283–10291.

Zucker RS. 1989. Short-term synaptic plasticity. Annu Rev Neurosci 12:13–31.